

6

REMOTE SENSING OF BODY SIGNS AND SIGNATURES

Prepared For Naval Medical Research and Development Command
National Naval Medical Center, Bethesda, Maryland 20814

AD-A162 106

DTIC
ELECTE
DEC 09 1985
S D

By James C. Lin and Karen H. Chan

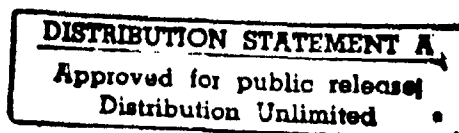
Department of Bioengineering (M/C 063)
The University of Illinois at Chicago
Box 4348
Chicago, Illinois 60680

DTIC FILE COPY

Contract No. N00014-82-C-0659

Scientific Report No. BES-5
October 1985

Final Report
August 1, 1982 through September 30, 1985



85 12 6 103

REMOTE SENSING OF BODY SIGNS AND SIGNATURES

By

James C. Lin and Karen H. Chan
Department of Bioengineering
University of Illinois at Chicago
Chicago, IL 60680

Abstract

This report describes the development of a microprocessor-based remote sensing system for non-contact detection of heart rate and respiration. Low power sinusoidal microwave signal at a frequency of 10.525 GHz is generated by a Gunn diode oscillator in an integrated Doppler transceiver. A standard gain horn is used to direct the microwave energy to the chest of a subject at a distance of a few centimeters. Since movements associated with the contraction of the heart and expansion of the lungs are translated into motions of the chest wall, the Doppler microwave reflected from the chest is processed to yield information on the frequency and regularity of these cardiopulmonary events.

The microprocessor-based battery-powered system is designed to provide continuous operation for approximately one hour. It allows selection of heart rate or respiration to be displayed on a 3-digit LCD. An analog output jack is provided for oscilloscope display or chart recording. The design range of heart rates is from 40 to 200 beats per minute and that for respiration is from 3 to 30 breaths per minute. The signal acquisition times for heart rate and respiration determinations is 12 and 48 seconds, respectively. Measurements on anesthetized laboratory rats and human volunteers showed good agreement between rates determined with the remote sensing device and conventional techniques, with correlation coefficients greater than 0.98.

Table of Contents

1.0	Introduction.....	2
2.0	Design Requirements.....	4
3.0	Operation Procedure.....	5
4.0	Microwaves.....	5
5.0	Analog Circuitry Section.....	7
5.1	Preprocessing.....	8
5.2	Digitization.....	9
6.0	Microprocessor Section.....	11
6.1	Microprocessor System Hardware.....	11
6.2	Software Development.....	13
6.2.1	Data Acquisition.....	13
6.2.2	Signal Analysis.....	14
6.2.3	Information Display.....	16
7.0	Evaluation and Conclusions.....	17
	References.....	20
	List of Tables.....	23
	List of Figures.....	24

Appendix

- A. Transceiver MA86501 Specification
- B. Schematic Diagram of Analog Circuitry
- C. Schematic Diagram of Digital Circuitry
- D. Program Listing
- E. Amplitude Response Curve for Filters

Accession For	
NTIS	CRA&I <input checked="checked" type="checkbox"/>
DTIC	TAB <input type="checkbox"/>
Unannounced <input type="checkbox"/>	
Justification	
By	
Distribution	
Availability Codes	
Dist	Avail. &/or Special
A-1	



REMOTE SENSING OF BODY SIGNS AND SIGNATURES

By

James C. Lin and Karen H. Chan
Department of Bioengineering
University of Illinois at Chicago
Chicago, IL 60680

Contract NO. N00014-82-C-0659

Scientific Report NO. BES-5
October 1985

Final Report
August 1, 1982 through September 30, 1985

Prepared For

Naval Medical Research and Development Command
National Naval Medical Center
Bethesda, Maryland 20814

1.0 INTRODUCTION

A portable non-invasive cardiopulmonary rate meter is needed for use in emergency situations in which direct contact with the patient is either impossible or undesirable. This report presents a device using Doppler microwaves to detect chest movement at a distance of a few centimeters from the subject. The information on the frequency and regularity of the heart and respiratory rate are extracted from the chest movement.

The lungs can be expanded and contracted by elevation and depression of the ribs to increase and decrease the anteroposterior diameter of the chest cavity. During expiration, the ribs slant downward, thus allowing the sternum to fall backward toward the spinal column. But, during inspiration, the rib cage is elevated. The ribs project directly forward so that the sternum moves forward away from the spine. The anteroposterior thickness of the chest can be 20 percent greater during maximum inspiration than during expiration.

The movements of the heart in the chest cavity and the intrinsic volume-pressure changes in cardiac chambers produce the motion of the chest wall. As the wave of excitation traverses the Purkinje system over the endocardial surface of the ventricles, the trabeculae carneae and papillary muscles begin to contract. With the onset of this contraction, the internal length of the heart decreases as the mitral valve is pulled toward the ventricular cavity. Simultaneously, there is an expansion of the circumference of the ventricular wall. The intracavitary pressure is generated and the circumference continues to increase in size until the movement of the aortic valve opening. This coincides with the maximal outward displacement of the chest wall produced by the heart. During the ejection phase, the circumference diminishes and the ventricular pressure continues to decrease until atrium filling begins. This causes the inward displacement of

the chest wall.

A variety of techniques have been developed over the years to record this chest movement and extract the respiratory and cardiovascular information from these signals. Among these are: strain gage and resistance pneumographs [1]; impedance pneumographs [2-4]; apexcardiograms [5,6].

Strain gage and resistance pneumographs measure the changes in the length of the chest. Body movements cause artifacts, which are dimensional changes unrelated to lung volume changes. The impedance pneumograph is reliable and extensively used, especially as an apnea monitor for prematurely born infants.

During inspiration, the lung tissue fills with air and becomes more resistive. Electrodes are placed on the chest wall of the patient. Detection can not be made without direct contact with the subject. An apexcardiogram measures the precordial movement caused by the left ventricular expansion and contraction. A microphone is usually put on the patient's chest to convert the mechanical movement into electrical signals. The system has a tremendous variation in sensitivity resulting from the application of different degrees of pressure on the skin through the microphone.

In addition, several successful experimental results of ventricular function and respiratory function measurement using the detection of chest wall motion with Doppler microwaves have been reported [7-14]. Microwaves can penetrate through clothing and do not require a coupling media. Therefore, this microwave approach overcomes some of the motion artifacts and variation in sensitivity which results when electrodes are strapped onto a patient.

The objective of this work is to design, build and test a prototype device that will detect chest movement. The design is limited to a device that will non-invasively measure the heart and respiratory rate at a distance of few centimeters from the subject. The device makes no attempt to examine the wave

shape nor to diagnose diseases. However, it is hoped that this prototype device demonstrates the feasibility of using Doppler microwaves as a method of measuring cardiopulmonary rates in a situation in which direct contact with the subject is either impossible or undesirable.

The design requirements and operation procedure for the cardiopulmonary rate meter are presented first, then each stage of the monitor will be described (Fig. 1). This description will include the microwave source used to detect the movement of the chest motion, analog signal preprocessing, analog to digital conversion and the controlling unit, an Intel 8085-based microprocessor system. The software involved in controlling data acquisition and analyzing the chest motion to give the cardiopulmonary rates is also discussed. Preliminary results are included to demonstrate the performance of the device.

2.0 DESIGN REQUIREMENTS

The device is designed to make cardiopulmonary rate measurements and to be operated by health professionals in either indoor or outdoor settings. This imposes some limitations to the device's size, weight, circuitry, choice of power and operation procedure. The device must be compact and light in weight (not more than 10 lbs.) so that it can be easily moved from location to location. The choice of hardware circuitry has to be optimal so as to consume minimum power. The device must be battery-powered and capable of providing continuous operation for at least one hour. Operational procedures have to be simple (an example is given below), and data easily acquired and processed. It must include warning lights to inform the operator of inadequate data. Switches need to be provided to allow selection for processing and displaying information on either the heart signal or the respiratory signal.

3.0 OPERATION PROCEDURE

1. Turn on the power switches at the back of the box and on the lower right-hand corner of the front panel.
2. Press down the corresponding switch for the desired channel to be processed.
3. Push the "RESET" switch on the front panel to clear the display and warning lights and to initialize the program counter of the microprocessor to begin execution at the beginning of the data acquisition routine.
4. Wait for the green "READY" LED to light up, which indicates completion of the reset routine.
5. Place the transceiver directly above (for supine position) or in front of (for standing or sitting position) the subject's sternum.
6. Press the "START" button to prompt the microprocessor to begin accepting data for processing.
7. The "READY" LED will extinguish at the completion of the data acquisition and the system will automatically process the data and display the desired information on the LCD.
8. Warning lights will indicate that inadequate data has been taken, informing the operator that the measurement must be repeated.

4.0 MICROWAVES

Microwaves are electromagnetic waves occupying the frequency range from 300 MHz to 300 GHz. They can be reflected and absorbed by different physical and biological objects. These modes of interaction depend on the dielectric constant and the orientation of both electric and magnetic fields of the incident waves, and the direction of propagation. No attempt has been made to discuss the topic of microwave interaction in this report. For more information, the reader can refer to references [15-18]. However, the factors

leading to the choice of the microwave input device, the transceiver, will be discussed. The relationship between the transceiver output and the chest motion will be explained briefly in this section of the report.

A x-band Doppler transceiver (MA86501) designed by Microwave Associates for speed measurement or motion sensing applications was selected (technical specifications are given in Appendix A). This transceiver consists of a fixed tuned CW Gunn diode oscillator and a Schottky Barrier mixer diode assembled into a compact waveguide package.

At this frequency (10.525 GHz), the reflection coefficient at an air-muscle or an air-skin interface is higher than 70% and the reflected power is about 50% of that on the interface. It indicates that transmission and reflection detection are equally efficient. The wavelength of the signal dictates the spatial resolution of the biological target of interest. The penetration depth, i.e., the distance through which the power density decreases to 14% of the incident power as the wave travels in the media, determines the site of motion detection (surface or depth). The wavelength in air for 10.525 GHz microwave is 2.8 cm and the penetration depth is about 0.03 cm [18]. The above characteristics of the signal allow the device to detect surface chest motion with reasonable spatial resolution.

Microwave radiation is considered a form of electromagnetic radiation. Under normal circumstances, microwave radiation is too low (1.24×10^{-3} eV/photon) to effect ionization, causing orbital electrons in the atoms of the material through which the waves are traveling to eject and become ions, or excitation, promoting orbital electrons to higher energy levels. It is also non-cumulative over time. A "safe" human exposure level has been established by the American National Standard Institute (ANSI) to control exposure duration and power density in order to prevent possible harmful effects on

human beings. The guideline for the frequency range 1500 MHz to 100 GHz is 5 mW/cm² (average over any 0.1 hour period) [18]. The power density, estimated by dividing the output power by the area that will be irradiated, is less than 1 mW/cm², and clearly meets the "safe" exposure standard for humans.

The transceiver is very easy to operate. The only requirements are to provide the recommended bias voltage across the bias and ground pins. The typical operating voltage is +8.5V while the typical operating current is 120mA. The output signal is presented at the IF output pin. The Gunn diode oscillator and the Schottky Barrier mixer diode are very sensitive to static charges. An enclosure is built to protect these diodes. Working in an anti-static workstation when soldering components onto the pin is highly recommended.

The relationship between the transceiver output and the movement of the chest motion is based on the well-known Doppler principles (microwave energy reflected by a moving target is shifted in frequency). The Gunn diode generated microwave energy is directed toward a moving target, the chest. The Schotky diode receives a reflected signal with a shift in frequency from the target. The mixer combines the transmitted and returned signal to produce the Doppler shift frequency signal which is proportional to the displacement of the target relative to the source of microwaves. Fig. 2 is a block diagram of the transceiver.

5.0 ANALOG CIRCUITRY SECTION

The output signal from the microwave transceiver, which is about 20mV peak-to-peak, must be preprocessed and digitized so that it can be analyzed by the microprocessor system. The preprocessing includes amplification and filtering. The amplification maximizes the dynamic range, while the filtering separates the heart and breathing signals. Then a multiplexer presents either

the heart signal or the breathing signal, held at two separate sample hold circuits (S/H), to an analog-to-digital converter (ADC) for digital coding. An explanation of the analog design is given in this section. For more detailed information and schematic diagrams, see Appendix B.

5.1 Preprocessing

Fig. 3 is a block diagram of the analog circuitry of the cardiopulmonary rate meter. The preamplifier stage is designed to provide proper impedance matching between the microwave transceiver and the rest of the circuits. The microwave transceiver is supplied with a 1000Ω load resistor from the mixer output pin to the ground pin to protect the mixer diode. The optimum intermediate frequency (IF) output load impedance specified by the manufacturer is 500Ω . Therefore the input impedance of this preamplifier stage must be 1000Ω . The preamplifier is a non-inverting amplifier with a gain of 2 (see Fig. 4). A 1000Ω resistor is placed across the positive terminal of the operational amplifier (op-amp) and ground. With this resistor in place, the amplifier has an input impedance of 1000Ω . The 1000Ω resistor on the transceiver is parallel with the 1000Ω input impedance of the amplifier and provides the optimum IF load.

The signal is then passed through a band-pass filter to eliminate the high frequency noise and to filter out the d.c. component of the transceiver output. The range of heart rates is from 40 beats/min to 200 beats/min, while the range of respiratory rates is from 3 breaths/min to 30 breaths/min. Therefore, the -3dB cutoff frequency at the low end of the filter is set to 0.03 Hz and that at the high end to 3.3 Hz. The band-pass filter is a combination of a 4th order Butterworth biquad low-pass filter and a 4th order Butterworth Sallen-Key high-pass filter (see Fig. 5). The Butterworth is characterized by having the flattest pass-band, but the transition between

passband and stopband is relatively slow. For a fourth order filter, the attenuation is approximately -24 dB/octave. These characteristics will ensure that the signal passed by the filter will be undistorted and that high frequency noise will be removed. The biquad circuit was chosen because of its significant tuning advantages and excellent stability characteristics, which are important in the cascading of several stages [19]. The Sallen-Key circuit allows the gain and frequency to be adjusted independently. The total gain for this stage is adjustable by the operator. The highest gain obtained is over 500, theoretically; however, it is limited by the frequency gain product of the op-am. A gain of 50 is usually used.

After this band-pass filter, the signal is fed into a parallel combination of a high-pass and a low-pass filter. The purpose of filtering stage is to separate the heart signal from the breathing signal. The low-pass filter is a 4th order Butterworth biquad filter with -3 dB cutoff at 0.5 Hz. The high-pass filter is a 4th order Butterworth Sallen-Key filter with -3dB cutoff at 0.6 Hz. The breathing signal is usually stronger than the heart signal. Therefore the low-pass filter, which outputs the breathing signal, has a gain of 2, and the high-pass filter, which outputs the heart signal, has a gain of 5.

Fig. 6-7 are examples of the breathing and heart beating patterns detected by the meter. A BNC output is provided by the meter to allow recording of the analog signal for permanent records.

5.2 Digitization

Fig. 8 shows a block diagram of the circuitry performing the digitization of the analog signal. It includes 2 sample holds, a multiplexer and an analog-to-digital converter. The Analog Device AD7574 is an 8 bit microprocessor compatible ADC. It employs the successive-approximation

technique to quantize the analog signal into an 8-bit digital code. The Datal Intersil SHM-IC-1 holds samples constant during the conversion period so that quantization will be accurate. The multiplexer AD7506 (Analog Device) connects the ADC to one of the two S/R outputs (one for the heart signal and one for the breathing signals).

The AD7574 (Fig. 9) operates from a +5 volts power supply and has a internal clock, an on-board comparator and interface logics. It is interfaced as a static RAM. A timing diagram is shown in Fig. 10. Upon receipt of a start command via the \overline{CS} pin, \overline{BUSY} goes low, indicating conversion is in progress. The internal asynchronous clock oscillator starts once the start command is received and ceases oscillating when conversion is complete. The clock oscillator requires an external R and C. The nominal conversion time is a function of the R and C values. $R_{CIK} = 127K$ and $C_{CIK} = 100$ pF are used to produce the 15 microseconds conversion time. For more detail, see [20]. The analog resolution is 0.078 volts for the ADC operating in bipolar mode.

The SHM-IC-1 (Fig. 11) is a self-contained device that requires only an external hold capacitor. The value is chosen by the user to achieve the desired speed and required accuracy. A 0.01 μ F capacitor is used to give an acquisition time of 10 microseconds and hold mode droop to only 5 mV/Sec maximum [21]. A polystyrene type capacitor is recommended because of its high insulation resistance and low dielectric absorption. The 10 μ s acquisition time plus the 15 μ s conversion time needed by the ADC is well within the time constraint set by the sampling frequency (80Hz/10Hz).

The AD7506 (Fig. 12) is a CMOS 16-channel analog multiplexer [20]. It switches a common output to one of 16 inputs, depending on the state of four address lines and an "ENABLE." It has both low R_{on} (ohmic resistance between the output and an addressed input) and power consumption. Two channels out of

16 available are used. The multiplexer was chosen not only because of its good quality but also because of its availability at the time of doing the design.

The analog circuitry explained up to this point is all that is needed to produce data that is of good resolution for the microprocessor system to analyze. The hardware and software design for the microprocessor system will be presented in the next section.

6.0 MICROPROCESSOR SECTION

The microprocessor section of the cardiopulmonary rate meter is the main controlling unit for data acquisition, signal processing and information display. The hardware design and the software development are presented in this section of the report.

6.1 Microprocessor System Hardware

The block diagram of the microprocessor system is shown in Fig. 13. Intel 8085A was selected as the central processing unit of the microprocessor system. 8085A is an 8-bit general purpose microprocessor designed as an enhancement of 8080A. It integrates the functions of clock generation, system bus control, interrupt priority selection, and execution of the instruction set in a single 40-pin DIP package. It requires only a single +5 volts supply. Its output signals are TTL compatible so that extra TTL buffering is not necessary. In addition, Intel has designed several peripheral components combining memory, Input/Output (I/O), and timer functions which can be directly interfaced to the multiplexed 8085 bus structure. With all these features, the number of components required for the system can be minimized and hardware development and debugging are simplified. The availability of a microcomputer development system, with an 8085 in-circuit emulator, which is a development aid for hardware and software debugging, contributed a major

consideration to the choice of the 8085 over other 8-bit microprocessors.

The hardware design follows closely the design recommendation by Intel Corp. in MCS-85 User's Manual [22]. The schematic diagrams are included in Appendix C. As mentioned above, 8085A is an 8-bit general purpose microprocessor (Fig. 14). The address and data buses of the 8085A are time multiplexed. ADO-AD7 are bidirectional lines which output the low order byte of memory addresses when "ALE" goes low. A8-A15 are output-only lines which carry the high order byte of memory addresses, which enable the CPU to access directly up to 64 K bytes of memory. It also generates control signals to select appropriate external devices, and functions to form READ and WRITE operations and also to select memory or I/O ports. The 8085A can address up to 256 different I/O locations (00 through FFH). There are two ways of addressing I/O devices: the I/O-mapped I/O (IO/M is used to distinguish between I/O and memory READ and WRITE cycles); and the memory-mapped I/O (IO/M is not used).

In the present system, 8K of EPROM (0000H-1FFFFH), and 4K of RAM (3000H-3FFFFH) memories, and 6 I/O-mapped I/O ports (see Table 1) were implemented. The memory chips used were Intel 8755A (2048 words x 8-bits EPROM with I/O) and 8185 (1024 words x 8-bits static RAM), which are designed for direct interface to 8085A. Corresponding address, data and control lines are compatible to the 8085A multiplexed bus structure. One 74138 (one-to-eight decoder) and a combination of NAND and OR gates are used to decode part of the address bus (A11-A15) and to generate chip selects for the memory and I/O ports connected to the 8085A (see Fig. in appendix C).

The 8085A incorporates a complete clock generator on its chip. A quartz crystal of 6.25 MHz is connected across pins X1 and X2 to establish timing for its operation. The buffered clock output (ClK out) is connected to all the

memory chips to synchronize all the activities.

The 8085 is not guaranteed to function properly until 10 milliseconds after the +5 volts supply (Vcc) reaches +4.75 volts. For this reason, a simple RC network is designed to keep the RESET IN low until 90 milliseconds after Vcc reaches +4.75 volts for both power up reset and manual reset. Following the reset signal, the 8085A begins executing instructions at location 0000H.

When the RESET IN signal goes low, the various signals and buses are floated. For this reason, pull-up resistors are provided for the main control signals, WR and RD, to avoid spurious selection when they are tri-stated. The unused control lines for interrupt and HOLD state generation (TRAP, InTR, RST 7.5, RST 6.5, RST 5.5 and HOLD) are grounded to avoid undesirable activity. For detailed information on the 8085A, see [22,23].

6.2 Software Development

A main program written in FORTRAN and subroutines in both FORTRAN and 8085 Assembly language have been written to perform data acquisition, signal analysis and information display. An explanation of the software development is presented in this section. For a more complete discussion of the programming methods, see Appendix D for the source listing.

6.2.1 Data Acquisition

The main program is for controlling the timing for each event. Upon initialization, the main program calls subroutine GETRDY. GETRDY clears the LCD display and the LED warning signals and then lights the "READY" LED to indicate that resetting of the system is complete and data acquisition may begin. This initialization is automatically done after a power up or after the "RESET" button is pressed. Once the transceiver is placed at the desired

position, the "START" button is pressed to prompt the CPU to begin the data acquisition.

The routine DATAIN does the actual data acquisition. The routine first switches on the desired channel according to its encoding. DATAIN then stores either twelve seconds of data in array HEART (960) or forty-eight seconds of data in array BREATH (480). It begins the acquisition of each element of HEART or BREATH by simulating a positive-going pulse for the digital control terminal of the S/H circuit. This signal tells the S/H to hold a sample for the ADC. The start conversion signal (refer to Fig. 10) is initiated by executing an I/O WRITE to port 00H which is occupied by the AD7574. Once the conversion is complete, a data READ is performed by executing an I/O READ instruction to the port 00H. The sample is in unsigned two's complement form and is stored in either the array HEART or BREATH. The next sample is held for the ADC after the appropriate delay. The delay is generated by the routine DELAY and ensures that the data is acquired at the rate of 80 Hz or 10 Hz for heart information and breathing information respectively. The sampling by the S/H and the conversion by the ADC is repeated until 960 samples for the HEART array or 480 samples for the BREATH array are acquired. The "READY" LED will then turn off by the DDone Routine signaling the operator that the acquisition is complete, the transceiver can be removed, and the signal analysis is being performed.

6.2.2 Signal Analysis

The routine starts by locating the peak of each cycle. A slope test is performed by comparing the slope approaching the pixel under consideration and the slope leaving the pixel. The direction of the slope approaching the pixel, P_1 is determined by the quantity of S_1 , where

$$S_1 = \sum_{k=1-4}^{1-2} (P_k - P_{k+2})$$

Similarly, the direction of the slope leaving the pixel is determined by S_2 , where

$$S_2 = \sum_{k=1}^{1+2} (P_k - P_{k+2})$$

Each slope in S_1 or S_2 is calculated not by the difference between two consecutive pixels, but rather by the difference between two consecutive pixels which are a pixel apart from each other. Three differences are summed together to give the value S_1 or S_2 . This improves the accuracy of the slope direction estimation in noisy signals. S_1 and S_2 will be negative for upslope, and positive for downslope. Points at which the signal changes from upslope to downslope are the local maxima.

The peak voltage of each cycle is adjusted to a value higher than one volt to improve the system dynamic range. Therefore, local maxima less than 0.5 V are mainly due to noise and motion artifact. They do not contribute significantly to the cardiopulmonary rate determination. A threshold of 0.5 V is set to eliminate these.

The program continues to search for the foot of each cycle. This is accomplished by proceeding back from the remaining local maxima to a point where the slope becomes negative. This minimum point is the foot, or the beginning of the cycle if its amplitude is less than a set point (zero is used for this program). The first maximum point from the foot is defined as the peak of the cycle (either systolic peak or the peak of inspiration) (see Fig. 15 for the steps in the logic of recognition).

Each cycle is analyzed as described above. Time difference between two

succeeding peaks is then calculated. Some disease states, such as immature beat, or any artifact, including noise, may cause unreasonably short periods. Occasionally, a heartbeat is missed or the breathing pattern is not regular. Some of those intervals are much longer than the others. A median of all the periods is used as a reference point to eliminate those extreme values (either too short or too long). An average is calculated from those within 5 points from the median.

6.2.3 Information Display

The final numerical values of the heart and respiratory rates are displayed on a liquid crystal display (LCD) (Fig. 16). LCDs are ideal for their low power consumption and rapid response times. The LCD chosen is an AND model FE0502 4 digit field effect liquid crystal display. This LCD allows for easy readability with its 17.8 mm character height, wide viewing angle, and high contrast ratio.

A four digit CMOS display decoder/driver (ICM7211AM) is used to drive the LCD. The ICM7211 provides a complete RC oscillator, back plane driver, and 28 segment outputs. An external capacitor is connected to the oscillator terminal so that the oscillator free-running frequency is kept below 125 Hz and the power consumption of the LCD is minimized. Unused segment terminals are connected to the backplane to avoid undesired characters or faint display.

The ICM7211 is controlled by the 8085A. Each digit to be displayed is written out to the LCD one at a time v/a port 08H. When the chip select lines $\overline{CS1}$, $\overline{CS2}$ (see Fig. 17) are driven low, the input buffer of the ICM7211 latches. The content of the latches is then decoded and stored in the output latches at the rising edge of $\overline{CS2}$. It is at this point that the digit is visible to the operator.

7.0 EVALUATION AND CONCLUSION

During the software development, three algorithms have been investigated. Autocorrelation was first implemented. The FORTRAN 80 in the Intel Intellect II Development System is an inefficient compiler. Any real number multiplication takes a long time to perform. The total time taken to acquire 480 data points (240 data/array) and analyze them to give the desired rate information was about 30 minutes. Even though the accuracy was very promising, the long processing time makes the algorithm impractical.

Another algorithm for finding the peak of each cycle reported in [24,25] was applied to the data. The heart signal is usually enveloped by the breathing artifact. The amplitudes of the peaks vary from cycle to cycle. The depth of breathing is not identical from breath to breath. A deeper breath will generate a stronger signal than a shallower one. Using the maximum point of the whole record of data to determine the threshold for identifying peaks of the cycles in the record is not reliable. Consequently, the performance of this algorithm is seriously affected by body motion and is dependent on the regularity of the signal amplitude of the chest movement.

The pattern recognition algorithm described in the previous section is designed for use in a portable 8-bit microprocessor-based system with 6K PROM and 1K RAM memories. The time for data acquisition and analysis is less than 90 seconds. The limited memories and the limited time for acquiring the rate information are the major constraints for developing the program. The accuracy is limited by its spatial resolution.

The algorithm was first tested on anesthetized rats (500 g, sodium pentobarbital, 40 mg/g Ip). These animals produced minimum motion artifacts and were breathing regularly. Seventeen readings were taken. Analog form of these chest movements signals were displayed on a storage oscilloscope and

rates were calculated from visually identified points on these records. The maximum error was found to be less than 3%. The scatter diagram for the meter and visually identified breathing rate data is shown in Fig. 17. The correlation coefficient was calculated to be 0.99.

The system was then tested on human subjects with the same evaluation method. The subjects were either sitting or lying down. Eleven readings for each of the heart rates and breathing rates were taken. The maximum % error for heart and breathing rates was 7% and 9%, respectively. The scatter diagrams for the meter and visually identified heart and breathing rate data are plotted in Figs. 18 and 19. Again, the correlation coefficients were found to be 0.98 and 0.99, respectively. One major problem encountered in testing human subjects was the difficulty in directing the microwaves to the heart. It is found that placing the transceiver directly in front of or above the sternum of the subject gives the best result.

The relation between heart signals detected by the cardiopulmonary rate meter and ECG signals is shown in Fig. 21. It can be seen that there is indeed a one-to-one correspondence between the heart signals from the meter (the mechanical events) and the ECG signals (electrical events). Time differences between two succeeding peaks of the heart signals and those between two consecutive R waves were measured and are given in Table 3. The mean, standard deviation and variance were calculated for both sets of data. They all indicate that the Doppler microwave technique is capable of producing results as reliable as the ECG signals.

The repeatability of the system was examined by sequential testing of the same subject. The subject was instructed to sit still on a stool and to breath normally during the test. The transceiver was clamped on a stand and was located at a distance of 2-3 centimeters from the sternum of the subject.

The analog signal from the meter was displayed on an oscilloscope to monitor the signal. The test was repeated 13 times. The subject was then instructed to measure the heart rate by carotid pulse palpation every 15 seconds for 13 times. The subject was sitting still and breathing normally during this part of the test. The readings from the meter and from palpation are given in Table 4. The mean, standard deviation and variance for each set of data were calculated. The variances associated with the meter for both cases are smaller than those due to palpation. These results indicate that the repeatability of the meter is comparable, at least, to sensing by palpation.

Different devices other than commercial transceivers as input device have also been investigated. A low-power, compact, dual frequency (2 GHz and 10 GHz) transmit/receive circuit using microstrip technology was built and tested [26]. The reflected signals from the two-frequency microwaves were sampled and compared and an optimum signal is chosen electronically. The preliminary results (Fig. 22) indicate that the dual frequency feature enables the system to detect chest wall movement of a person more efficiently with either light clothing or thick and wet clothing. However, the sensitivity of the circuit needs to be improved. Further investigation in this area will likely enable the device to become more powerful as a noninvasive, noncontact cardiopulmonary rate meter under different kinds of environmental conditions.

In conclusion, the microprocessor-based cardiopulmonary rate meter offers a method to measure the heart and respiratory rates through non-contact and noninvasive modes.

References

1. Das, D. "Pulmonary instrumentation." Tompkins, Willis J. and Webster, John edited, Design of Microprocessor-based Medical Instrumentation, N.J.: Prentice-Hall Inc., pp. 27-29, 1981.
2. Stein, I.M. and Shannon, D.C., "The pediatric pneumograph: a new method for detecting and quantitating apnea in infants," Pediatrics, vol. 55, pp. 599-603, 1975.
3. Steinschneider, A., "A re-examination of the apnea monitor business," Pediatrics, vol. 58, pp. 1-5, 1976.
4. Schmalzel, J.L., Gallagher, R.R. and Barquest, J.M., "An impedance pneumograph utilizing microprocessor-based instrumentation," Biomed Sci. Instrum. vol. 13, pp. 63-68, 1977.
5. Tafur, E., Cohen, L.S. and Levice H.D., "The normal apexcardiogram," Circulation, vol. 30, pp. 381, 1964.
6. ___, "The normal and abnormal apexcardiogram," Am. J. Cardiology, vol. 8, pp. 368, 1963.
7. Lin, J.C., Kiernicki, J., Kiernicki, M. and Wollschlaeger, P.B., "Microwave apexcardiograph," IEEE Trans on Microwave Theory and Techniques, vol. MTT-27, No. 6, pp. 618-620, June, 1979.
8. Lin, J.C. and Salinger, J., "Microwave measurement of respiration," in Proc. IEEE International Microwave Symposium, pp. 285-287, 1975.
9. Lin, J.C., Daws, E. and Majcherek, J., "A non-invasive microwave apnea detector," in Proc. San Diego Biomed. Symp., vol. 30, pp. 441-443, 1977.
10. Lin, J.C., Microwave propagation in biological dielectric with application to cardiopulmonary interrogation. Unpublished text. Bioengineering Department, University of Illinois, Chicago, IL, 1983.
11. Pedersen, P.C., Johnson, C.C., Durney, C.H. and Bragg, D.E., "An

investigation of the use of microwave radiation for pulmonary diagnosis," IEEE Trans Biomed. Eng., vol. 223, p. 410, 1976.

12. Bragg, D.G., Durney, C.H., Johnson, C.C. and Pedersen, P.C., "Monitoring and diagnosis of pulmonary edema by microwaves: A preliminary report," Investigative Radiol., vol. 12, p. 289, 1977.
13. Hoshal, G., Siegel, M. and Zapp, R., "A microwave heart monitor and life detection system," in IEEE Frontiers of Engineering and Computing in Health Care-1984, pp. 331-333.
14. Lin, J.C., "Noninvasive measurement of respiration," Proc. IEEE, vol. 63, p. 1530, 1975.
15. Schwan, H.P. and Piersol, G.M., "The absorption of electromagnetic energy in body tissues, Part I: Biophysical aspects," American Journal Physical Medicine, vol. 33, pp. 372-404, 1954.
16. Lin, J.C. Microwave Auditory Effects and Applications, Springfield, IL, Charles C. Thomas, 1978.
17. Johnson, C., and Guy, A., "Non-ionizing electromagnetic wave effects in biological materials and systems," Proceedings IEEE, vol. 60, No. 6, pp. 692-718, June, 1972.
18. "ANSI Approves New Safety Standard," Bioelectromagnetics Society Newsletter, (34):1-2, Oct., 1982.
19. Thomas, L.C., "The Biquad-Part I: Some practical design considerations," IEEE Trans. Circuit Theory, CT-18, pp. 350-357, May, 1971.
20. Analog Devices, Data-Acquisition Data-Book, vol. I, Integrated Circuits, pp. 16-9-16-12, 11-113-11-120, 1982.
21. Datel Intersil, Data-Acquisition Component Handbook, pp. 212C-215C.
22. MCS-80/85 Family User's Manual, Santa Clara, CA: INTEL, 1979.
23. Osborne, A., An Introduction to Microcomputers: Volume II Some Real

Products, Berkeley: Adam Osborne and Associates, Inc., 1977.

24. Lee, J.Y. "A microprocessor-based non-invasive arterial pulse wave analyzer," M.S. Thesis, University of Illinois, Chicago, 1983.

25. Lee, J.Y. and Lin, J.C., "A microprocessor-based non-invasive arterial pulse wave analyzer," IEEE Trans. on Biomedical Engineering, vol. BME-32, no. 6, pp. 451, June 1985.

26. Popovic, M.A., Chan, K.H., and Lin, J.C., "Microprocessor-based noncontact heartrate/respiration monitor," in IEEE Frontiers of Engineering and Computing in Health Care, p. 754-757, 1984.

List of Tables

- Table 1. Input/output port assignment for the microprocessor system
- Table 2. Statistical evaluation between computer and visual determinations.
- Table 3. Statistical comparison between Doppler microwaves and ECG methods.
- Table 4. Statistical comparison of the cardiopulmonary rate meter and the pulse palpation measurements.

List of Figures

- Fig. 1. Block diagram of the cardiopulmonary rate meter.
- Fig. 2. Block diagram of the MA86501 transceiver.
- Fig. 3. Block diagram of the preprocessing circuit.
- Fig. 4. The preamplifier.
- Fig. 5. Block diagram of the band-pass filter.
- Fig. 6. Recording of breathing pattern (10:1 attenuation probe used during measurement).
- Fig. 7. Recording of heart beating pattern (10:1 attenuation probe used during measurement).
- Fig. 8. Block diagram of the digitizing circuit.
- Fig. 9. Circuit diagram of ADC with external reference.
- Fig. 10. Timing diagram for control of ADC.
- Fig. 11. Circuit diagram of S/H circuit.
- Fig. 12. Functional block diagram of AD 7506.
- Fig. 13. Block diagram of microprocessor system.
- Fig. 14. Pin out diagram for 8085A.
- Fig. 15. Summary of basic steps in the pattern recognition program.
- Fig. 16. Circuit diagram of the LCD and ICM 7211 display driver/decoder.
- Fig. 17. Timing diagram for control of LCD display by the microprocessor.
- Fig. 18. Scatter diagram for the meter and visually identified breathing rate data.
- Fig. 19. Scatter diagram for the meter and visually identified heart rate data.

- Fig. 20. Scatter diagram for the meter and visually identified breathing rate data.
- Fig. 21. Simultaneous recordings of the heart signals from chest movements and corresponding ECG signals.
- Fig. 22. Recordings of breathing and heart beathing patterns (10:1 attenuation probe used during all measurements).
- Fig. 23. Circuit diagram for fourth-order Butterworth Biquad low-pass filter.
- Fig. 24. (Same as Fig. 23).
- Fig. 25. Circuit diagram for fourth-order Butterworth Sallen-Key high-pass filter.
- Fig. 26. (Same as Fig. 25).
- Fig. 27. Schematic diagram for the digital circuit-I.
- Fig. 28. Schematic diagram for the digital circuit-II.
- Fig. 29. Schematic diagram for the digital circuit-III.
- Fig. 30. Amplitude response curve for the low-pass filter cut off at 3.3 Hz.
- Fig. 31. Amplitude response curve for the low-pass filter cut off at 0.5 Hz.
- Fig. 32. Amplitude response curve for the high-pass filter cut off at 0.6 Hz.
- Fig. 33. Amplitude response curve for the high-pass filter cut at 0.03 Hz.

Table 1: Input/Output port assignment
for the microprocessor system.

Port 00H	Analog-to-Digital Converter
Port 01H	Digital control for S/H BUSY signal from ADC
Port 08H	LCD display
Port 09H	LED warning lights
Port 10H	Front panel switches

Table 2: Statistical Evaluation Between Computer and Visual Determinations

<u>Measurements</u>	<u>Correlation Coefficient</u>	<u>Max Z Error</u>	<u>Mean Z Error</u>
Rat breathing rates	0.99	2.8	1.2
Human heart rates	0.98	7.0	2.1
Human breathing rates	0.99	9.0	3.1

Table 3: Statistical Comparison Between Doppler Microwaves and ECG Methods

<u>Doppler Microwaves Method</u>		<u>ECG Method</u>	
<u>periods in sec</u>	<u>heart rates in beats/min</u>	<u>periods in sec</u>	<u>heart rates in beats/min</u>
0.85	71	0.85	71
0.85	71	0.85	71
0.875	69	0.875	69
0.85	71	0.85	71
0.85	71	0.85	71
0.90	67	0.90	67
0.875	69	0.875	69
0.85	71	0.85	71
0.875	69	0.85	71
0.875	69	0.875	69
0.875	69	0.875	69
0.85	71	0.85	71
0.85	71	0.85	71
Mean	70	Mean	70
S.D.	1.30	S.D.	1.30
Var	1.57	Var	1.57

Table 4: Statistical Comparison of The Cardiopulmonary Rate Meter and the Pulse Palpation Measurements

<u>Cardiopulmonary rate meter</u> <u>Measurement</u>		<u>Pulse palpation</u> <u>Measurement</u>	
<u>Subject 1</u> beats/min	<u>Subject 2</u> beats/min	<u>Subject 1</u> beats/min	<u>Subject 2</u> beats/min
69	84	68	76
68	86	72	80
70	78	68	76
72	78	72	76
71	86	72	76
72	86	68	76
71	76	68	84
73	79	64	84
71	86	72	84
69	86	72	88
65	87	68	84
70	87	72	88
70	83	72	84
Mean 70	83	70	82
S.D. 2.06	4.00	2.64	5.04
Var 3.92	14.79	6.44	23.48

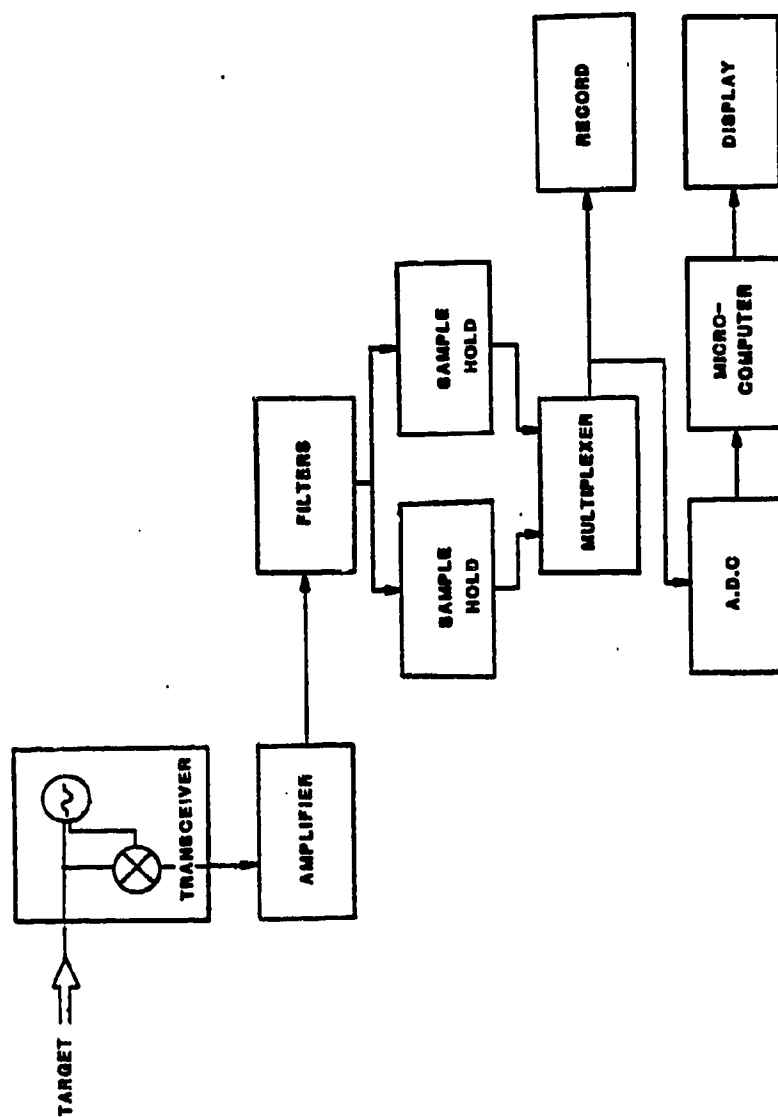


Fig. 1 Block diagram of the cardiopulmonary rate meter

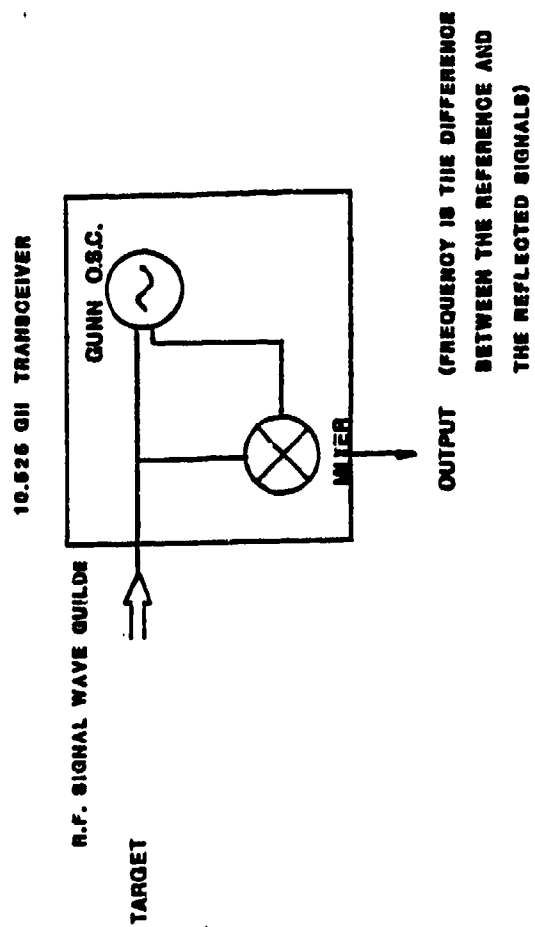


Fig. 2 Block diagram of the MA86501 transceiver

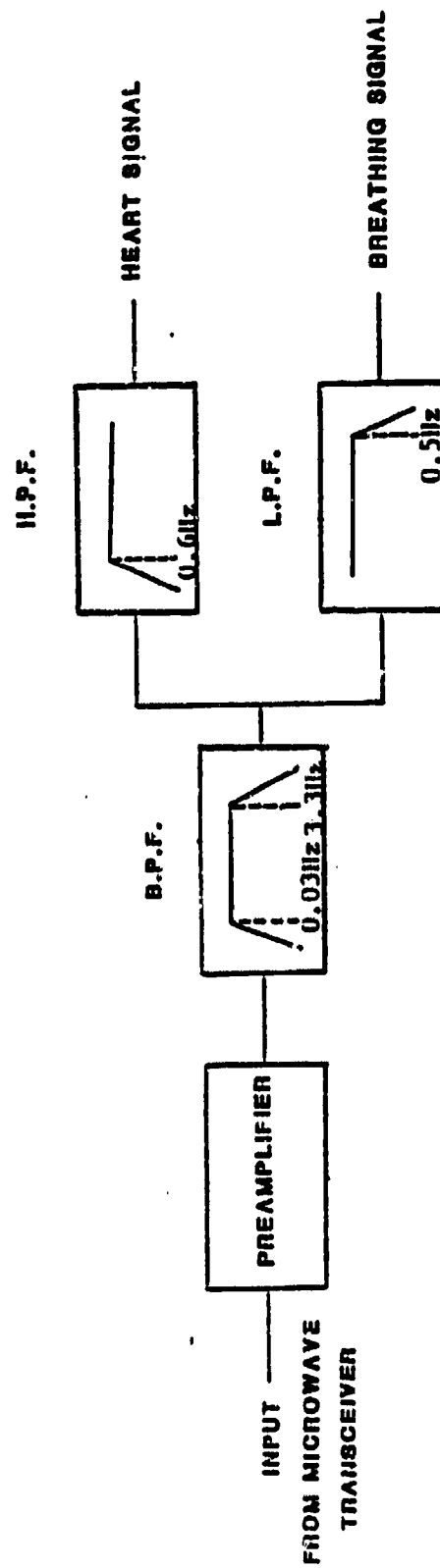


Fig. 3 Block diagram of the preprocessing circuit

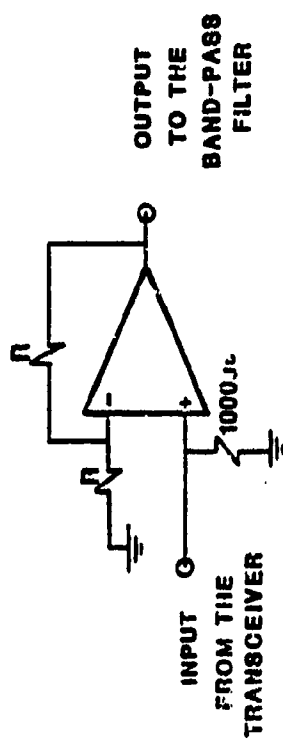


Fig. 4 The preamplifier

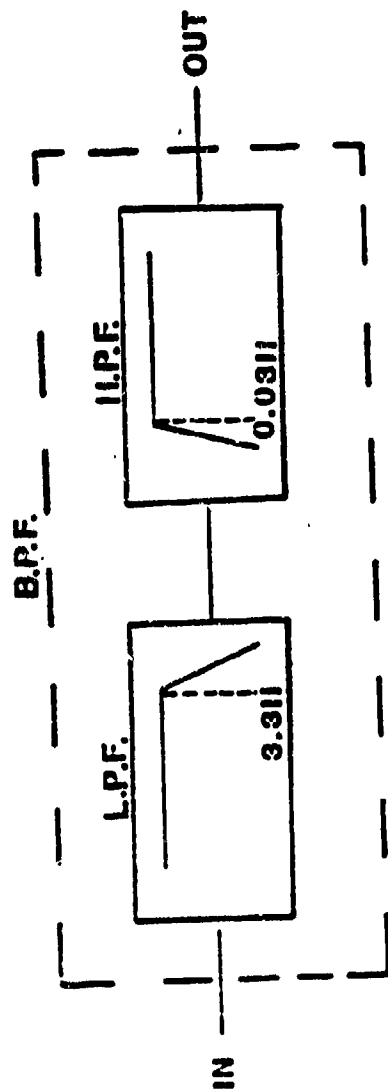


Fig. 5 Block diagram of the band-pass filter

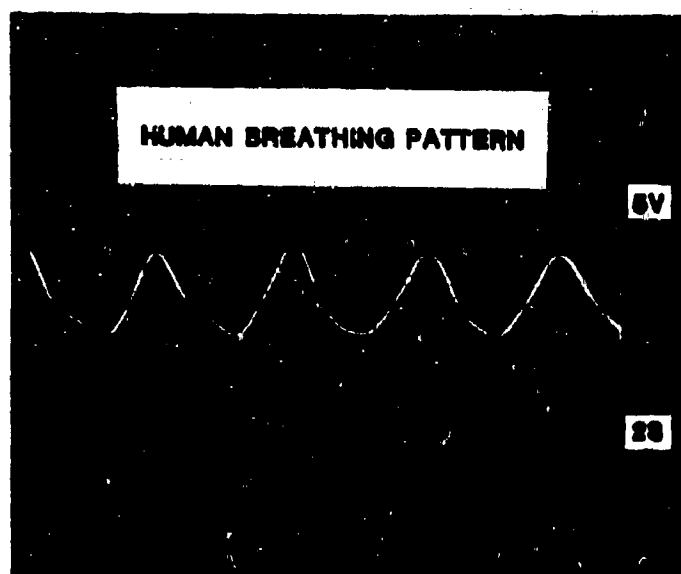


Fig. 6 Recording of breathing pattern (10:1 attenuation probe used during measurement)

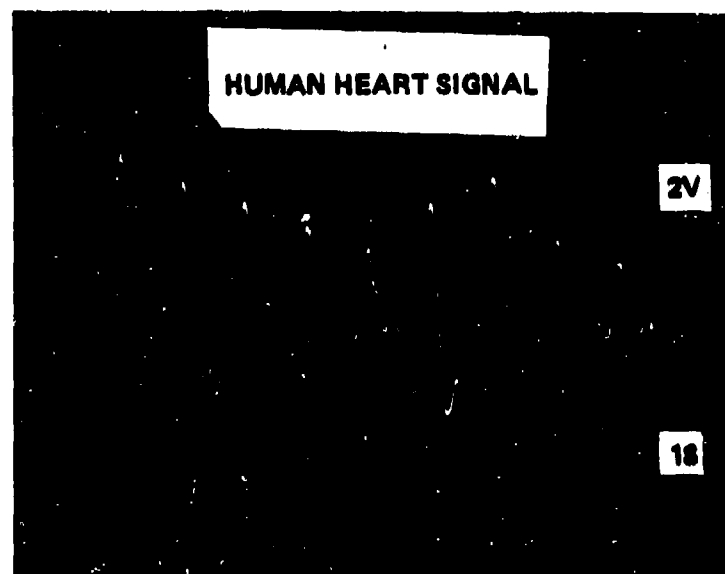


Fig. 7 Recording of heart beating pattern (10:1 attenuation probe used during measurement)

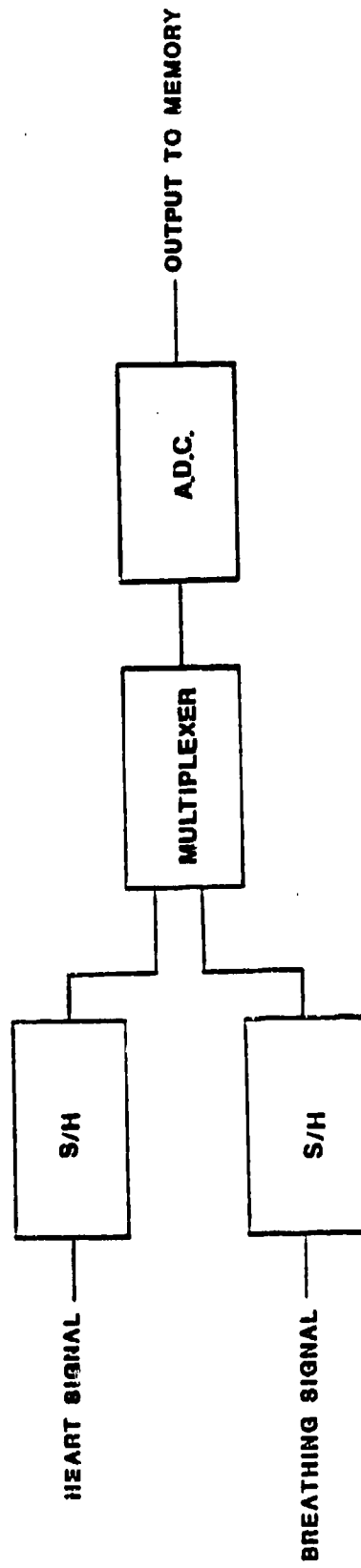


Fig. 8 Block diagram of the digitizing circuit

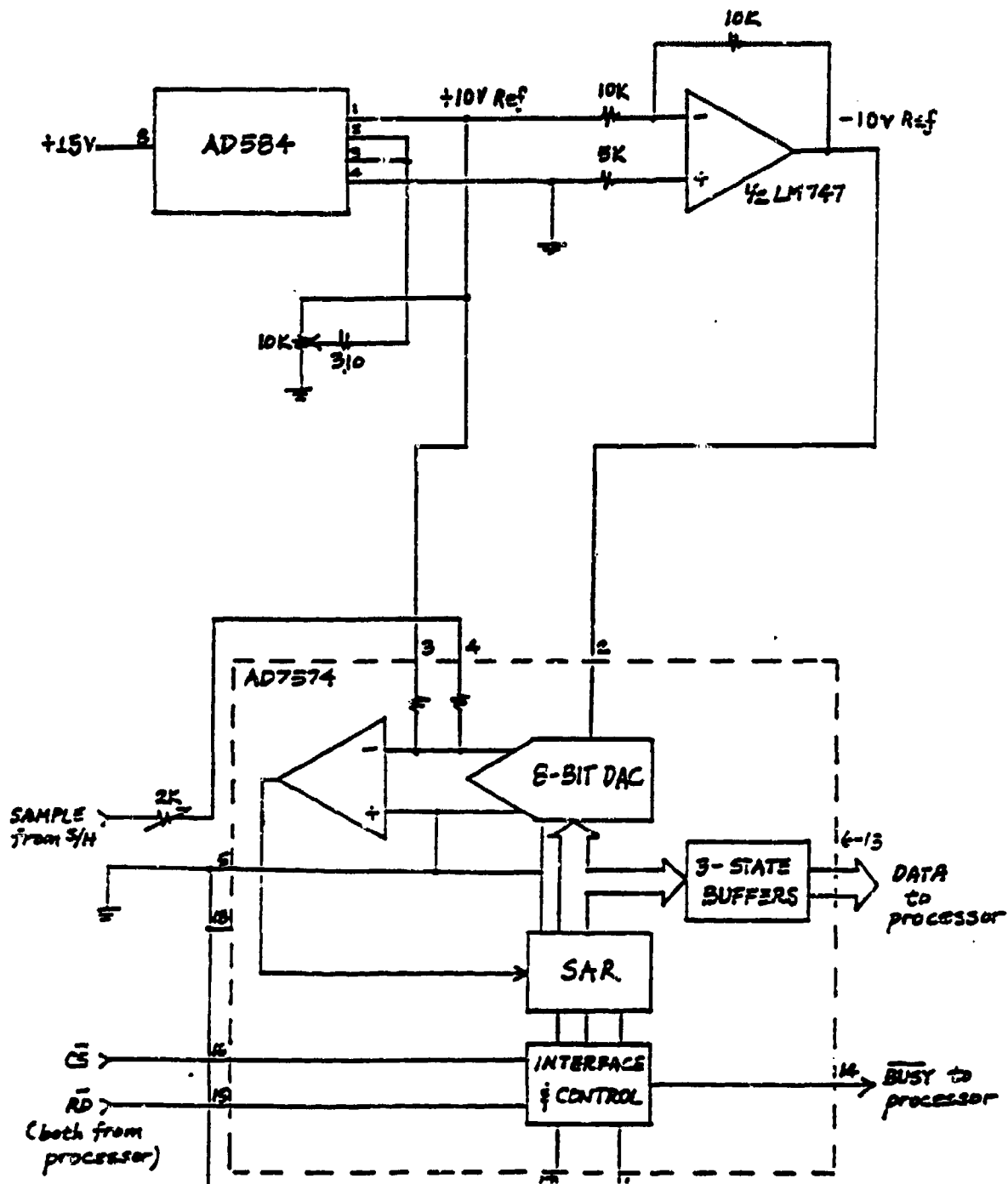


Fig. 9 Circuit diagram of ADC with external reference

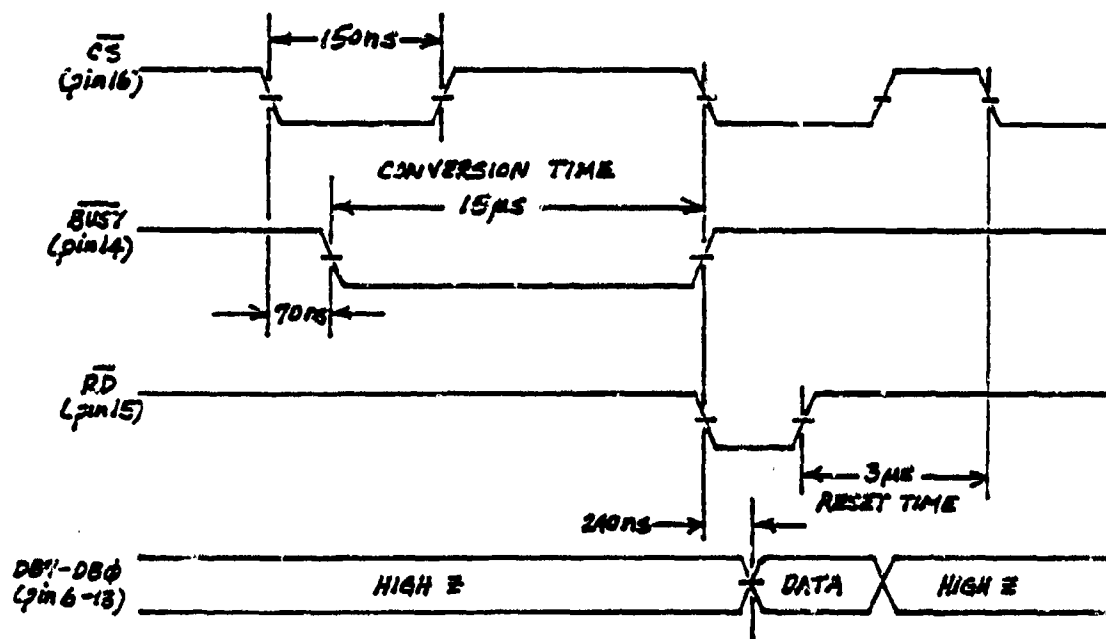


Fig. 10 Timing diagram for control of ADC.

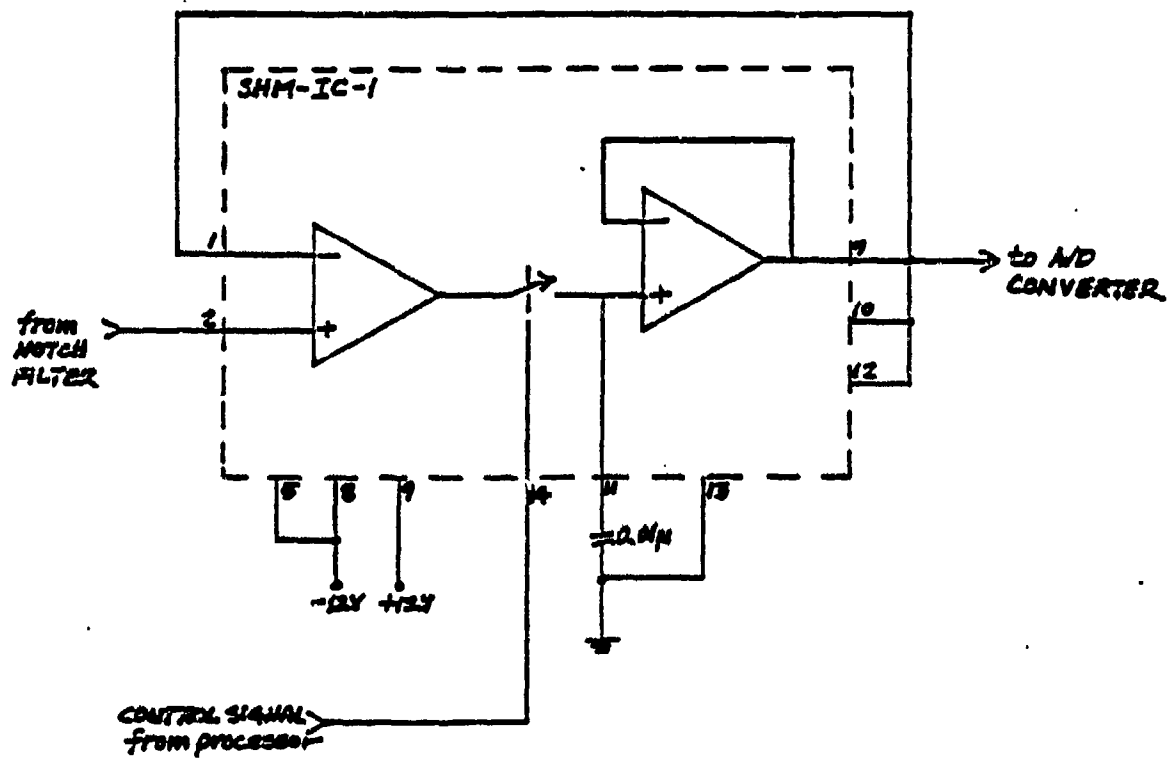


Fig. 11 Circuit diagram of S/H circuit

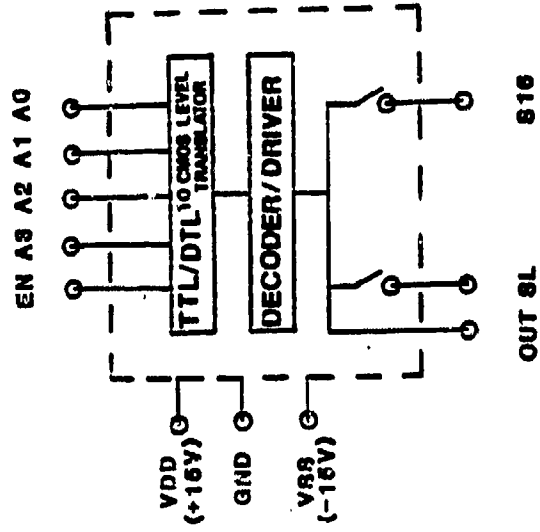


Fig. 12 Functional block diagram of AD 7506

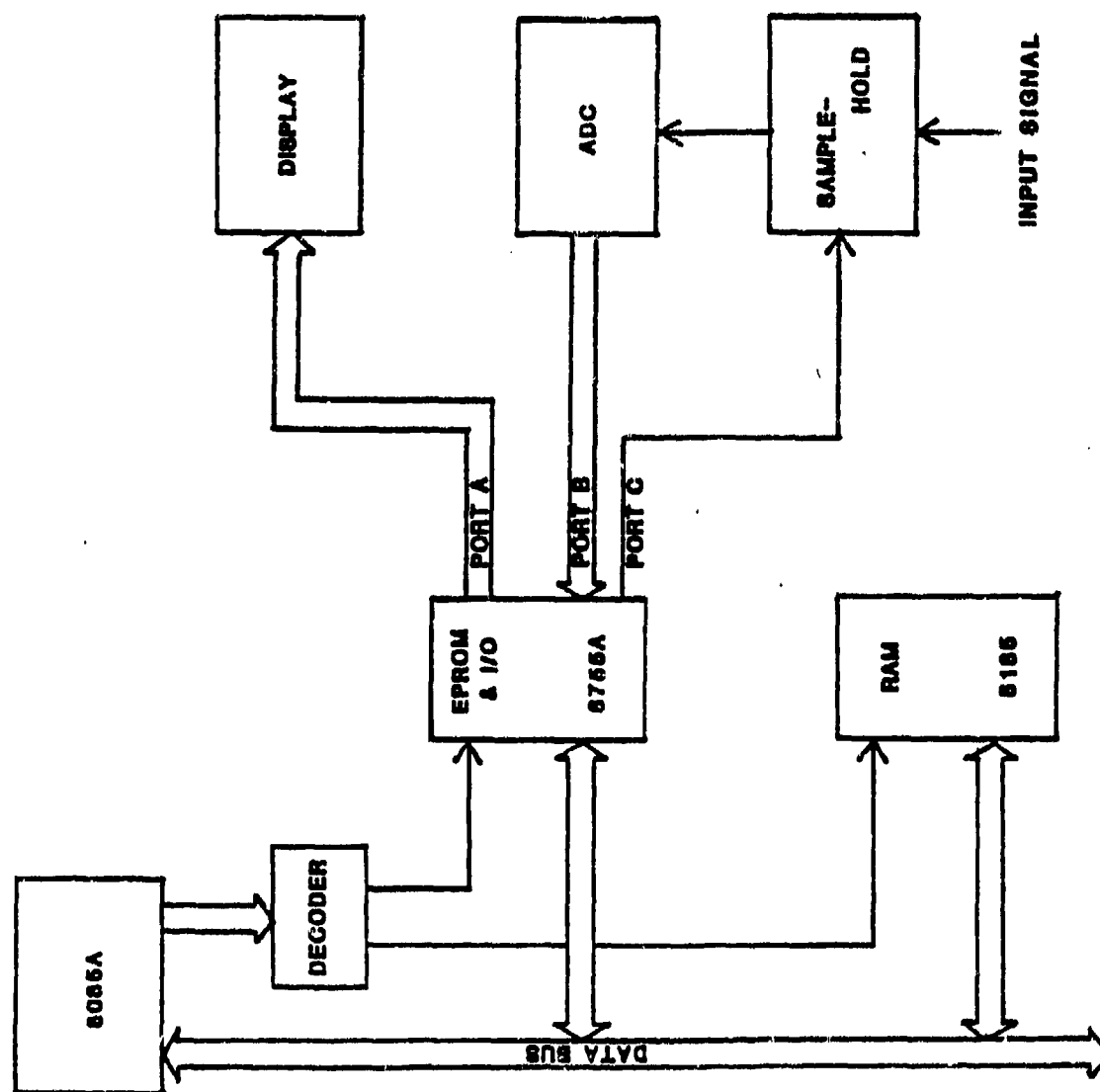


Fig. 13 Block diagram of microprocessor system

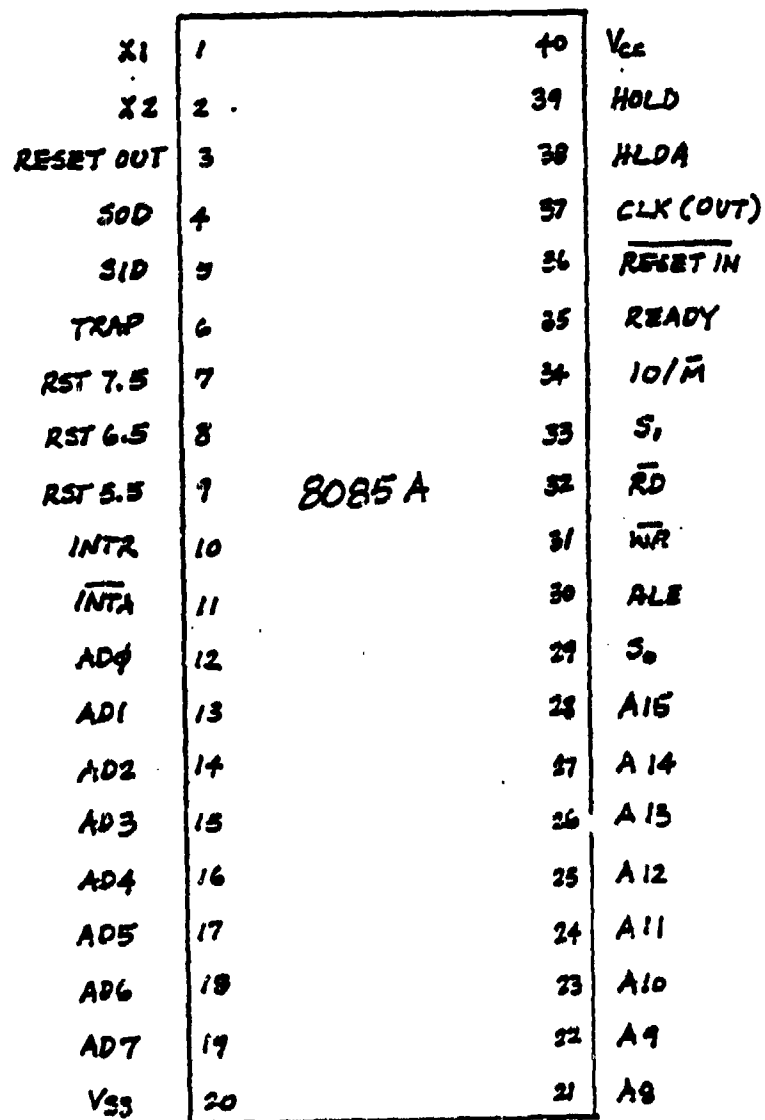


Fig. 14 Pin out diagram for 8085A

STEPS IN THE LOGIC OF RECOGNITION

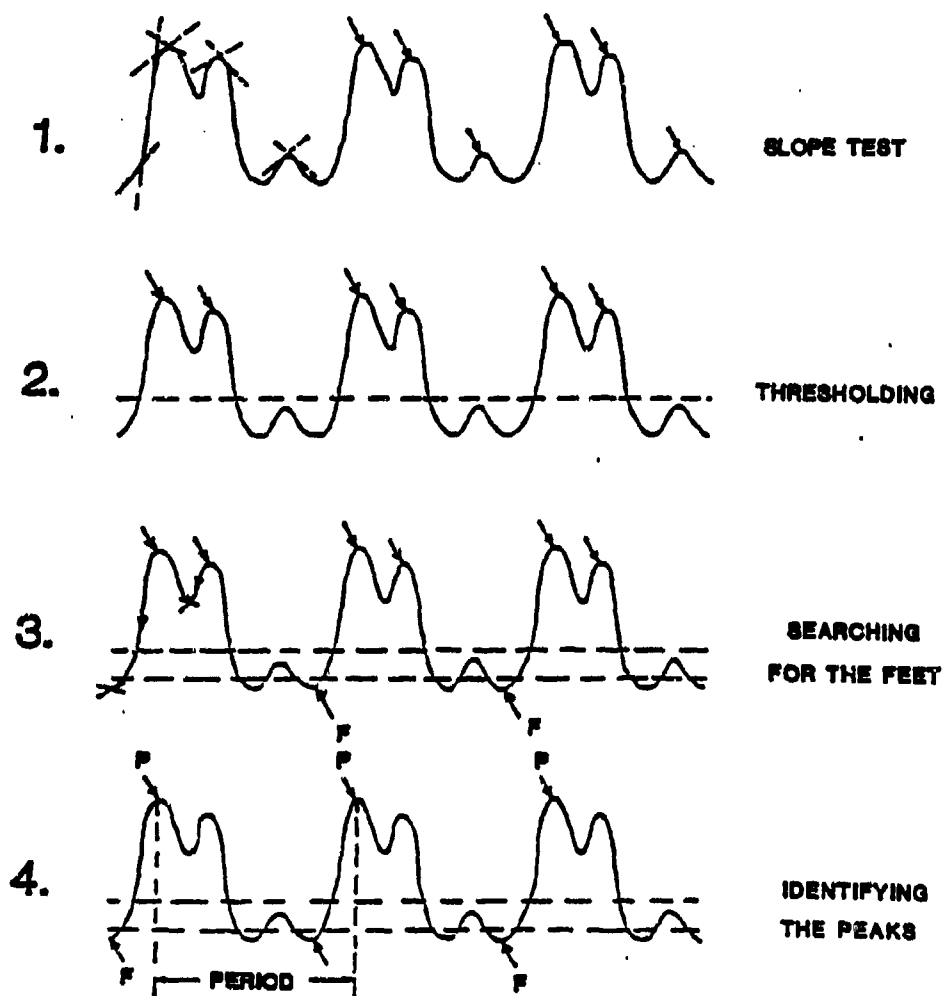


Fig. 15 Summary of basic steps in the pattern recognition program

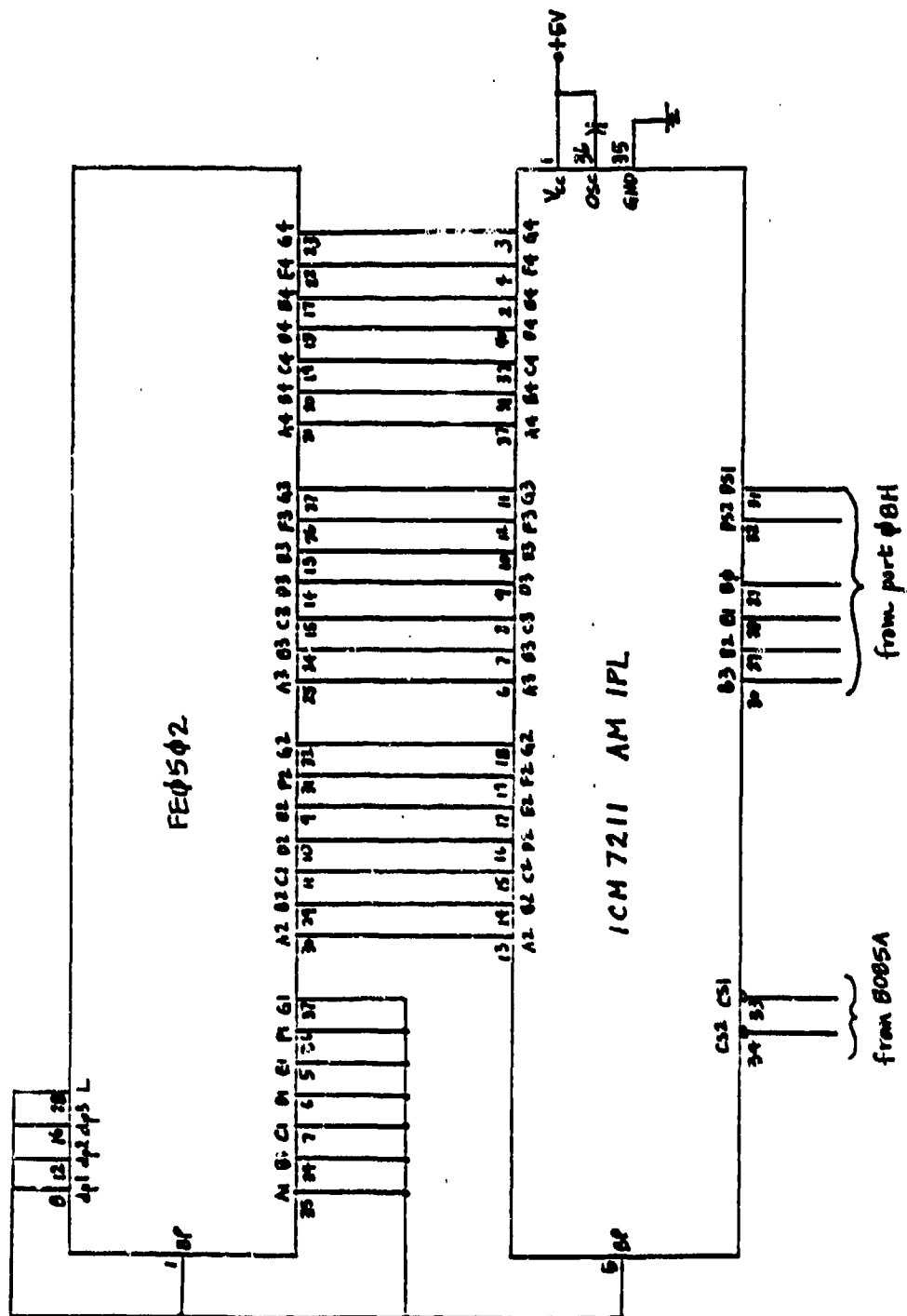


Fig. 16 Circuit diagram of the LCD and ICM 7211 display driver/decoder

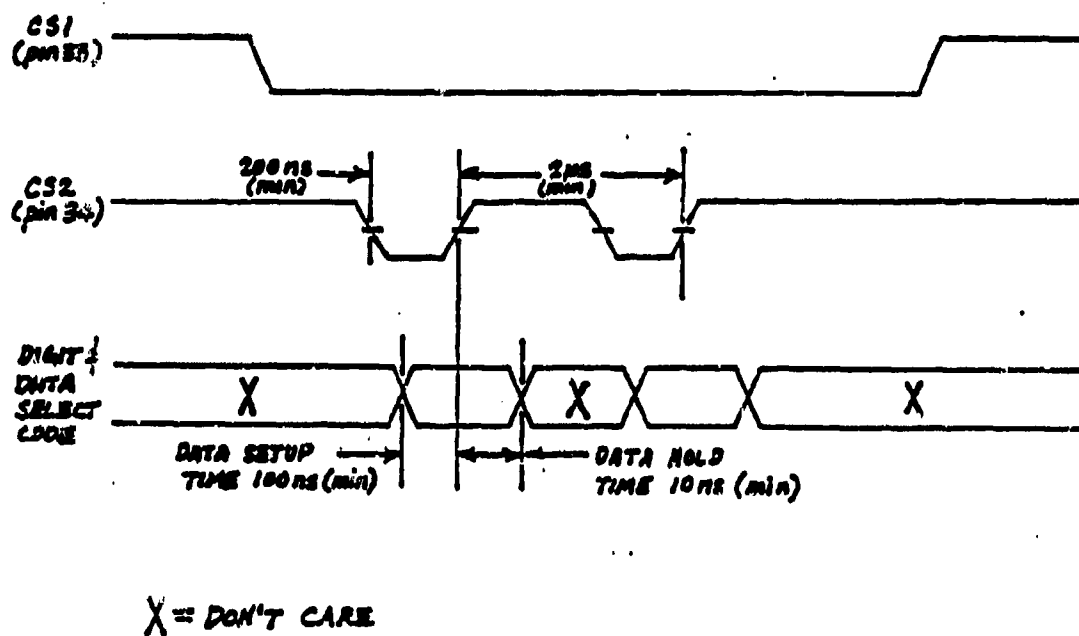


Fig. 17 Timing diagram for control of LCD display by the microprocessor

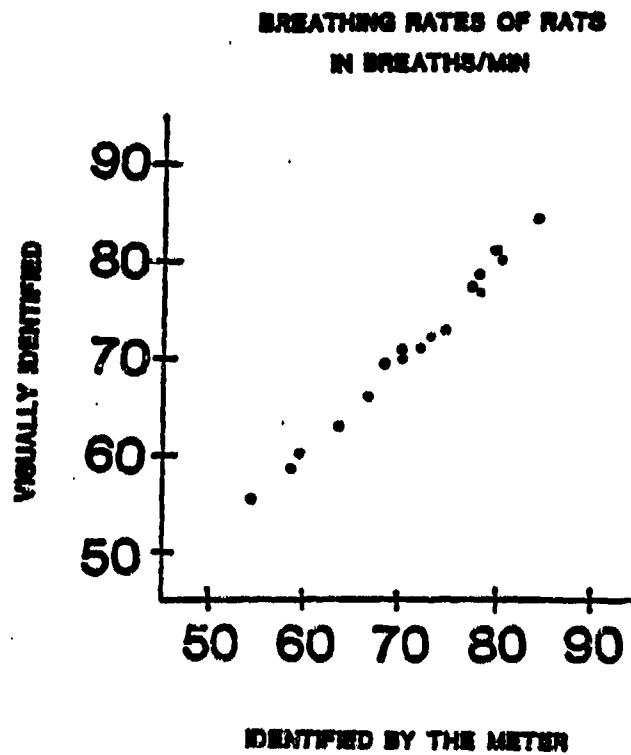


Fig. 18 Scatter diagram for the meter and visually identified breathing rate data

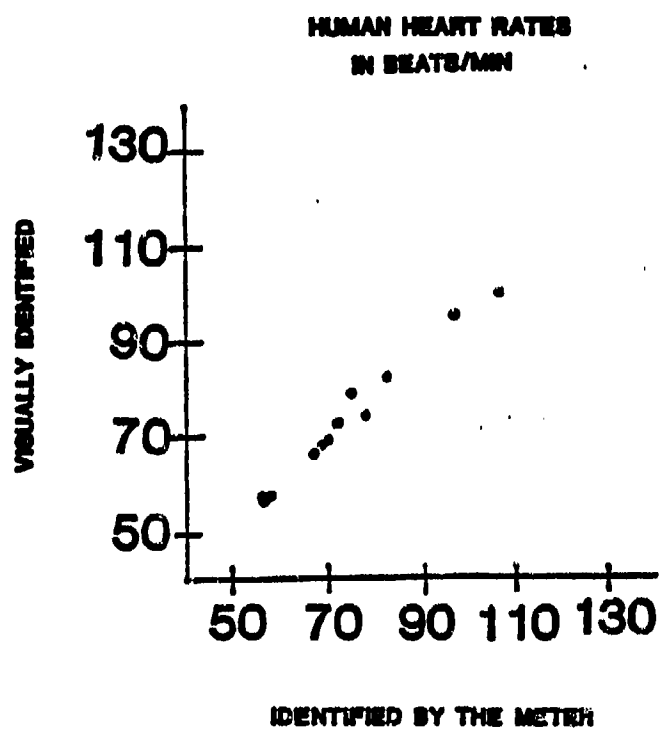


Fig. 19 Scatter diagram for the meter and visually identified heart rate data

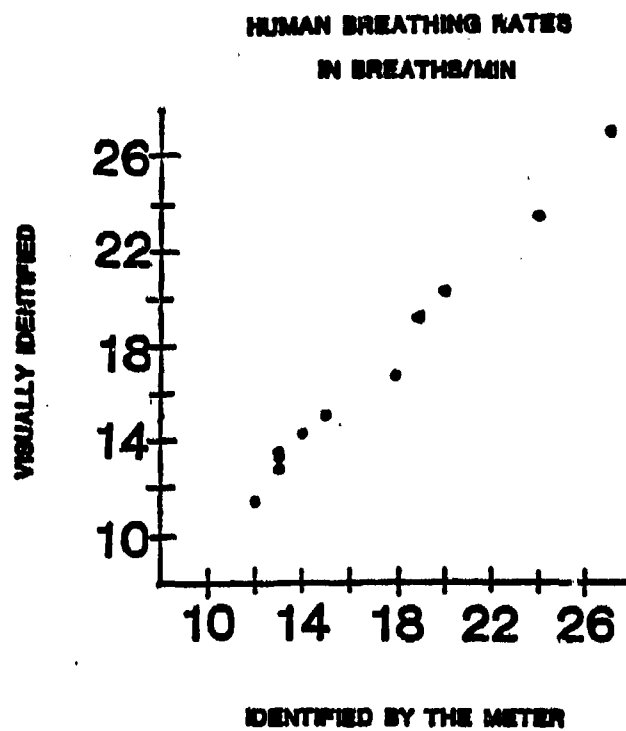


Fig. 20 Scatter diagram for the meter and visually identified breathing rate data

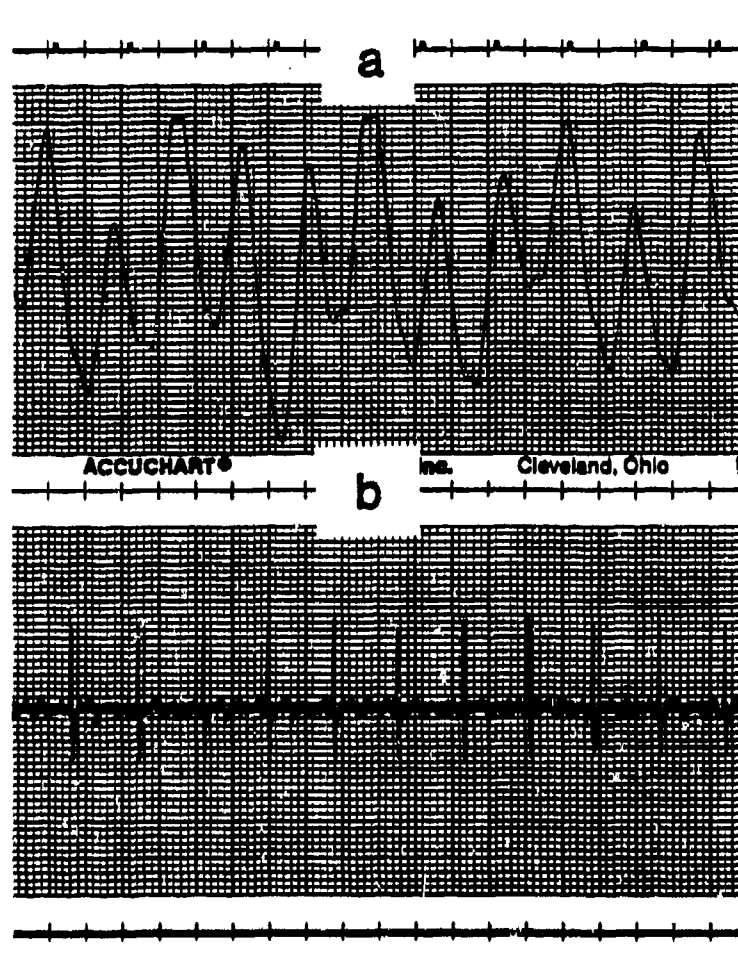


Fig. 21 Simultaneous recordings of the heart signal from chest movements and its corresponding ECG signals

BREATHING PATTERN

A female with
summer clothing



A female with
winter clothing

HEART BEATING PATTERN

A female with
summer clothing



Fig. 22 Recordings of breathing and heart beating patterns
(10:1 attenuation probe used during measurements)

Appendix A
Transceiver MA86501 Specification



MA-36501

Low Cost Doppler Transceiver

Description

The MA-86501 microwave Doppler transceiver is a low cost sensor designed for any speed measurement or motion sensing application. It provides an audio output signal whose frequency is proportional to the velocity of an object moving toward or away from the antenna.

Each transceiver consists of a Gunn oscillator and mixer assembled into a compact waveguide package. The standard model employs a fixed tuned CW oscillator and Schottky Barrier mixer diode. The mixer diode is field replaceable.

Applications

This transceiver is specifically designed for application in CW Doppler radar systems, speed radars, intrusion alarms, traffic control, braking systems, industrial process controls and other motion detecting systems.



Features

- LOW COST
- HIGH SENSITIVITY
- INTEGRATED ASSEMBLY
(INCLUDES MIXER DIODE)
- MEETS FCC PART 15 AND/OR PART
89 AND 93 REQUIREMENTS

M/A-COM GaAs PRODUCTS, INC.

Burlington, Massachusetts 01803 ■ Telephone (617) 272-3000 ■ TWX: 710-332-6789 ■ Telex: 94-9464

Bulletin No. 7614D

SPECIFICATIONS

Electrical Characteristics

Center Frequency	10.525 GHz
Mechanical Tuning Range	± 25 MHz
Power Output	5 to 10 mW typical @ 25°C Flange Temp.
Frequency Stability	40 PPM/°C Max. between end points
Spurious, harmonic	-35 dBm
Non-harmonic	-50 dBm
Detector Sensitivity	-55 dBc minimum for 10 Hz to 150 Hz IF bandwidth of
Operating Voltage	-7.5 Volts typical
Operating Current	20 mA typical 50 mA max.

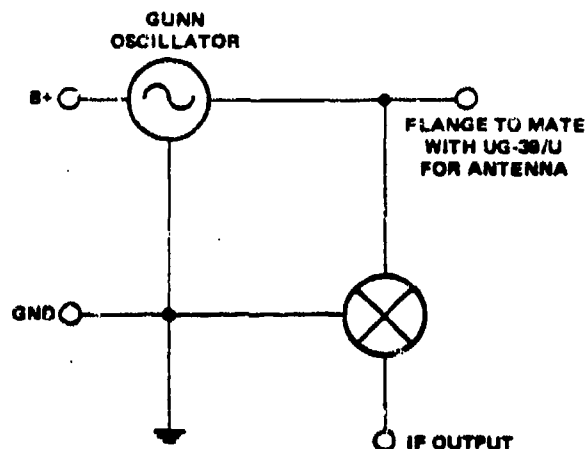
Mechanical Characteristics

Input Connector	Solder Lug
RF Output	To mate with UG-39/U Flange

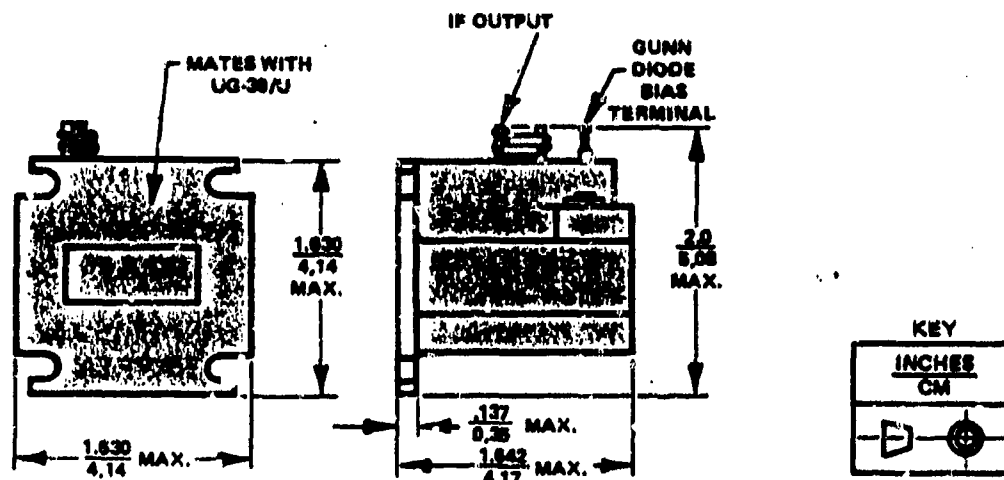
Environmental Characteristics

Operating Temperature	-30° to +70°C
-----------------------	---------------

BLOCK DIAGRAM



OUTLINE DRAWING



APPLICATION NOTES

- Optimum IF load impedance is 500 ohms. All units are supplied with a 1000 ohm load resistor in place to protect the mixer diode. The recommended input impedance of the IF amplifier is 1000 ohms. The two 1000 ohm resistors in parallel provide the optimum load.
- RF power for the L.O. signal is obtained directly from the transmitter signal as it "passes" the detector diode near the output flange. However, a large antenna mismatch will reflect sufficient power to alter the detector bias. The detector bias is factory adjusted to be suitable for an antenna VSWR up to 1.5:1. If the desired antenna has a larger VSWR it is recommended a simple matching screw be placed in the antenna structure to reduce its VSWR.
- Each unit is factory tuned to the specified frequency within ± 5 MHz. Operating frequency can be mechanically adjusted over a range of ± 25 MHz.
- Scale factor is 31.4 Hz per mile/per hour of radial velocity.
- An operating voltage of -7.5 volts typical is available.
- Spurious and harmonic emission levels are determined in a radiative measurement as required under part 15 of the FCC rules and regulations.
- An electrolytic capacitor (between 1 and 10 μ F) is required between the Gunn bias terminal and ground.

Appendix B

Schematic Diagram of Analog Circuitry

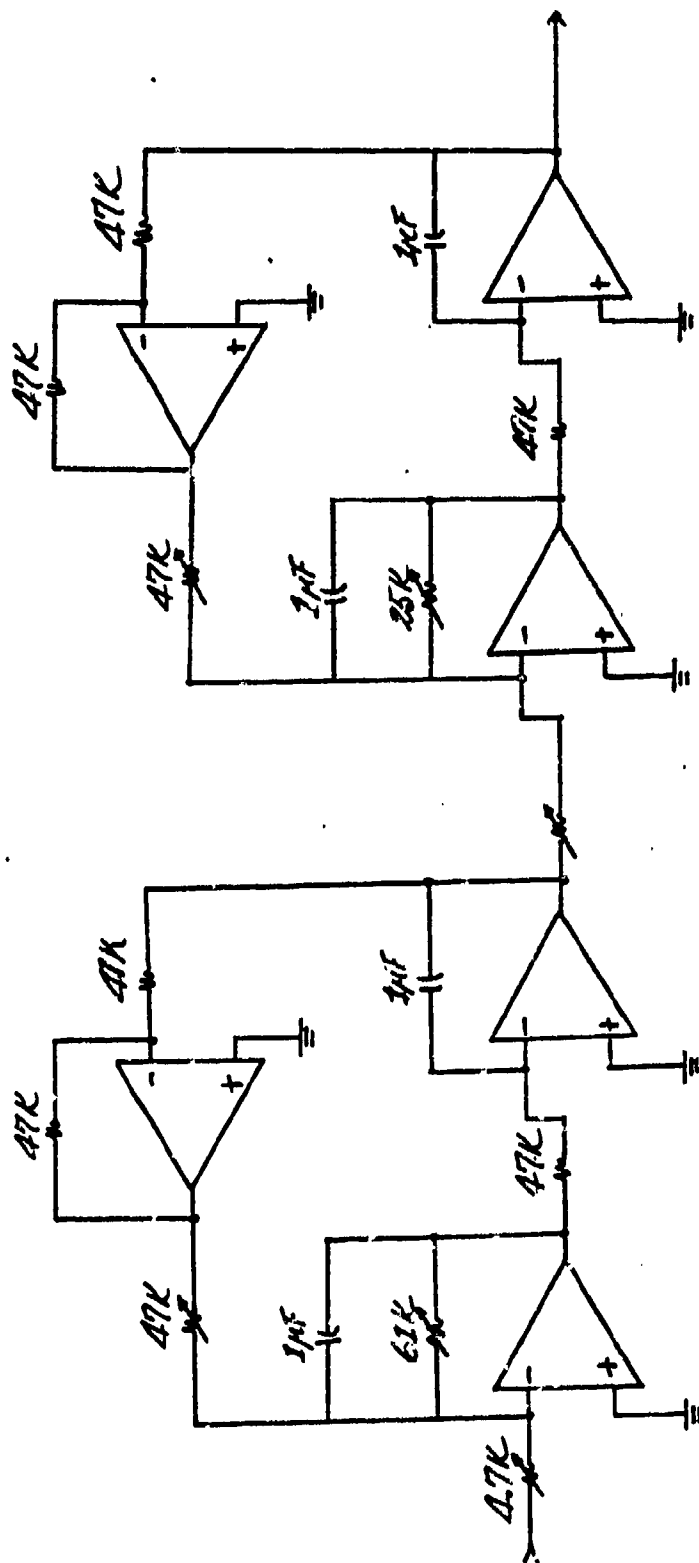


Fig. 22 Circuit diagram for fourth-order Butterworth Biquad lowpass filter
(cut-off frequency = 3.3 Hz)

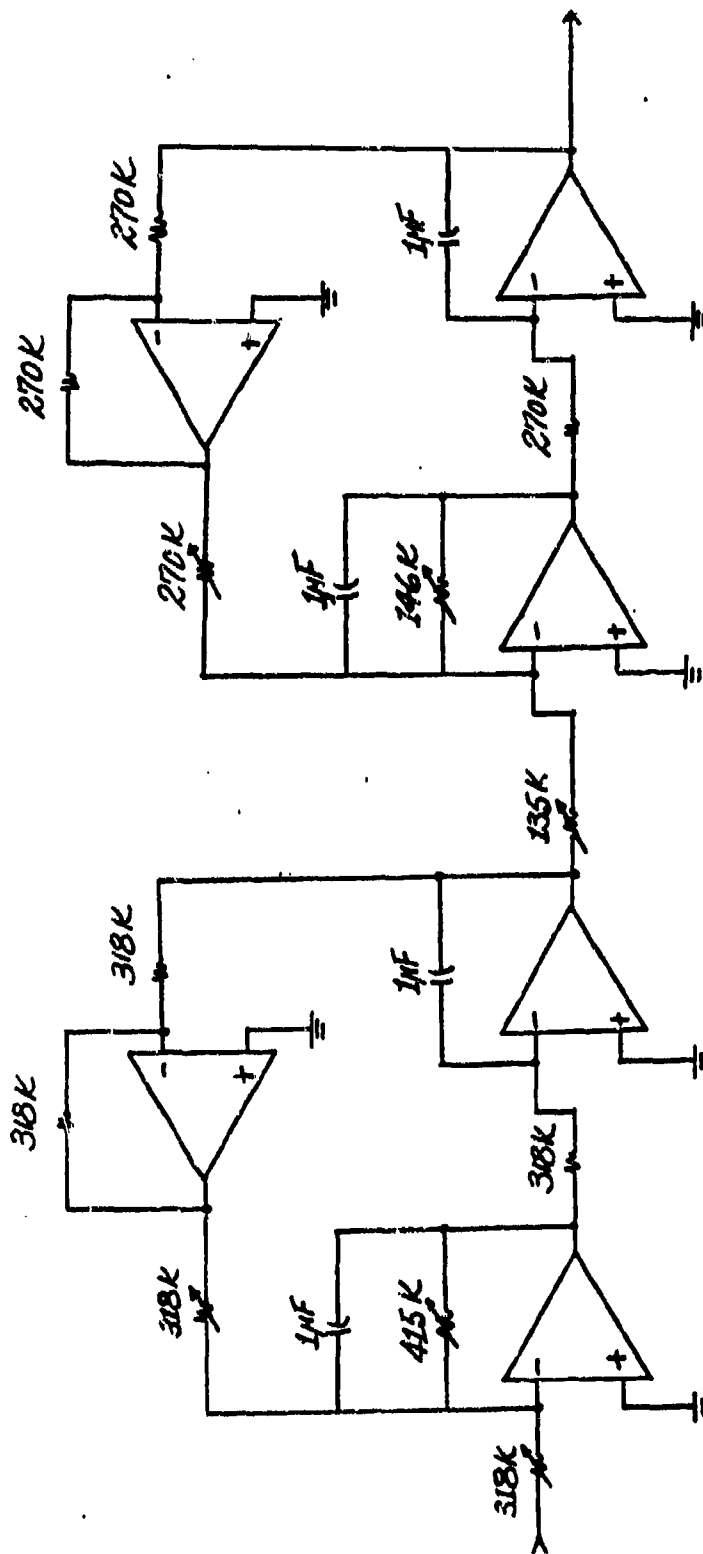


Fig. 24 Circuit diagram for fourth-order Butterworth Biquad low-pass filter
(cut-off frequency = 0.5 Hz)

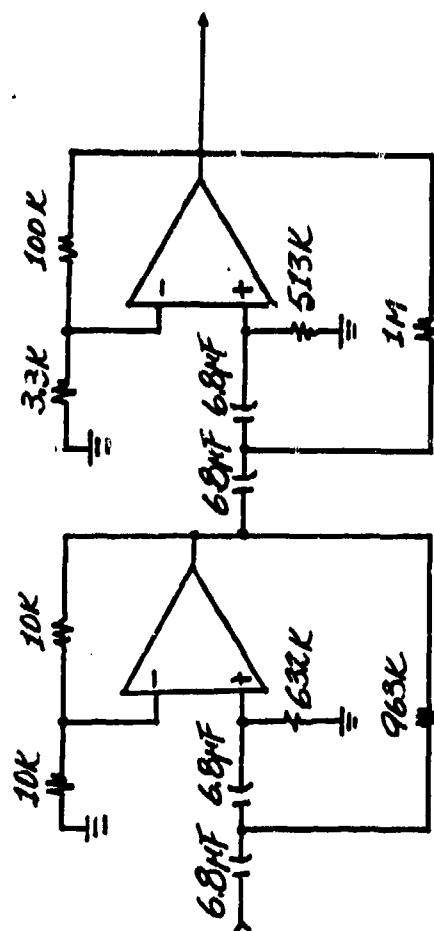


Fig. 25 Circuit diagram for fourth-order Butterworth Sallen-Key high-pass filter (cut-off frequency = 0.03 Hz)

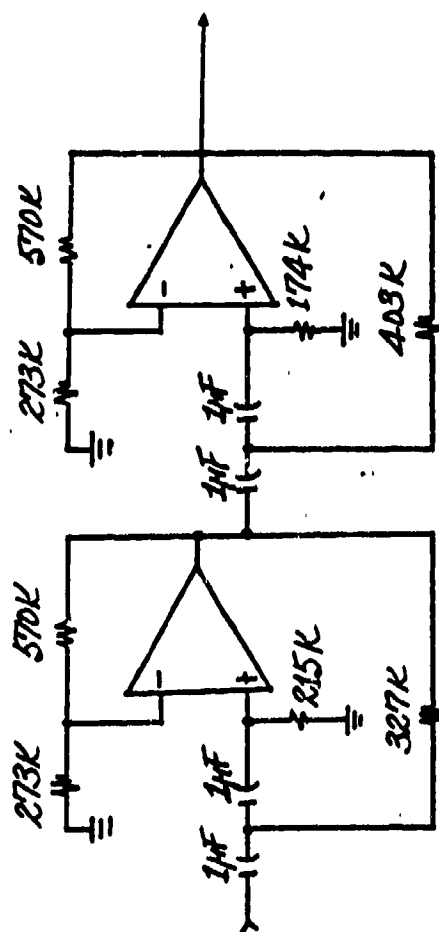


Fig. 26 Circuit diagram for fourth-order Butterworth Sallen-Key high-pass filter (cut-off frequency = 0.6 Hz)

Appendix C

Schematic Diagram of Digital Circuitry

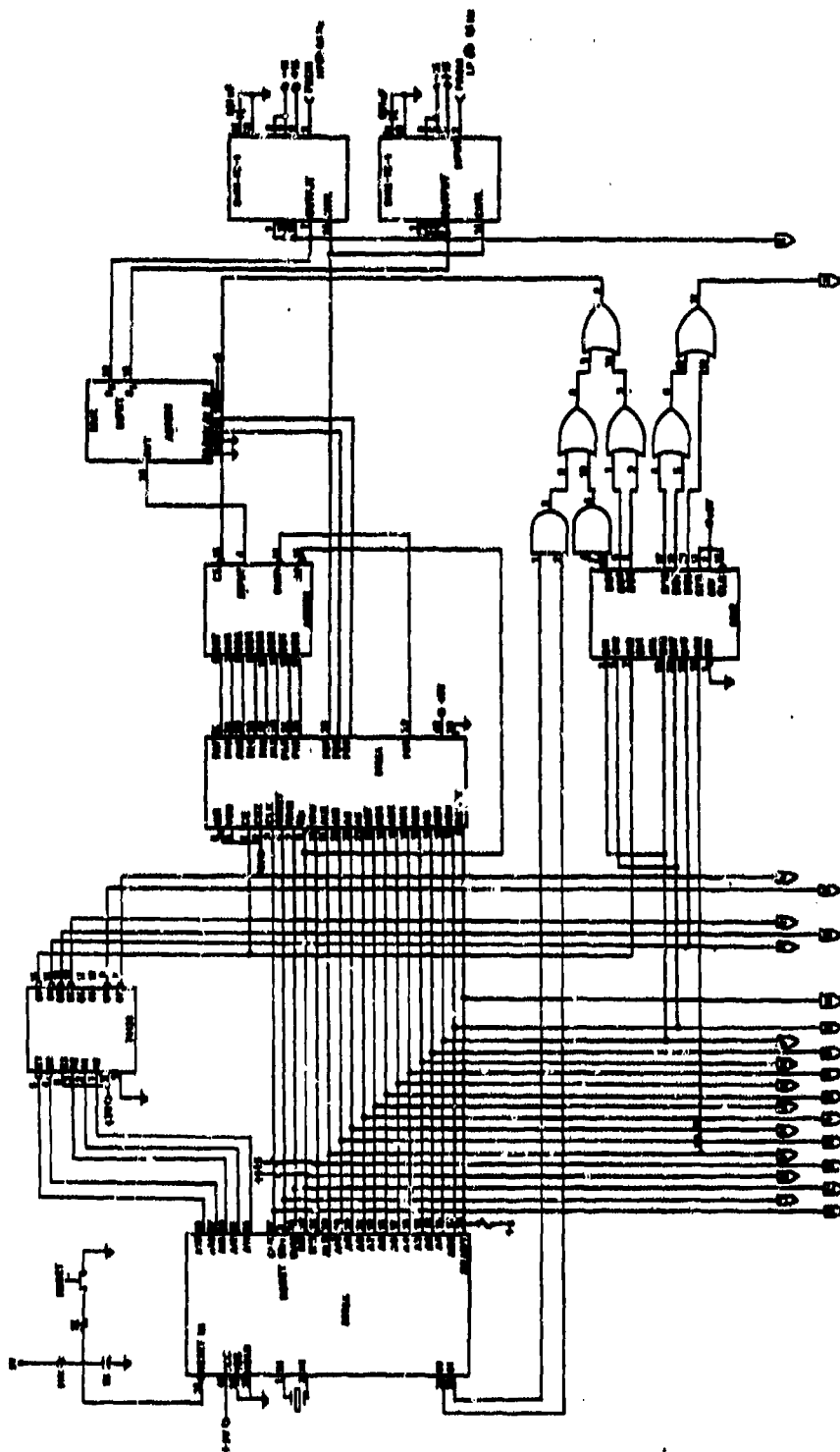


Fig. 27 Schematic diagram for the digital circuit-I

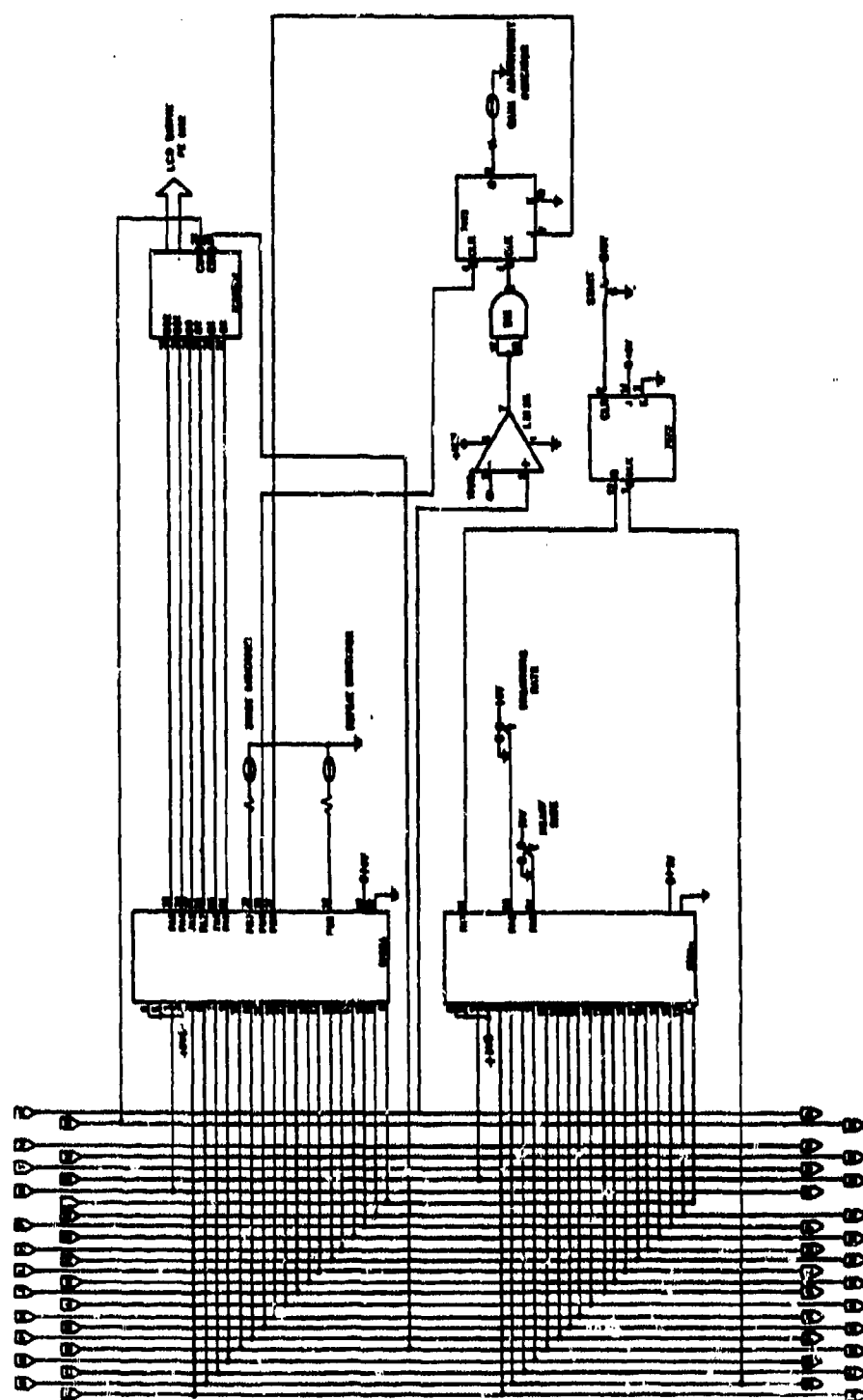


Fig. 26 Schematic diagram for the digital circuit-II

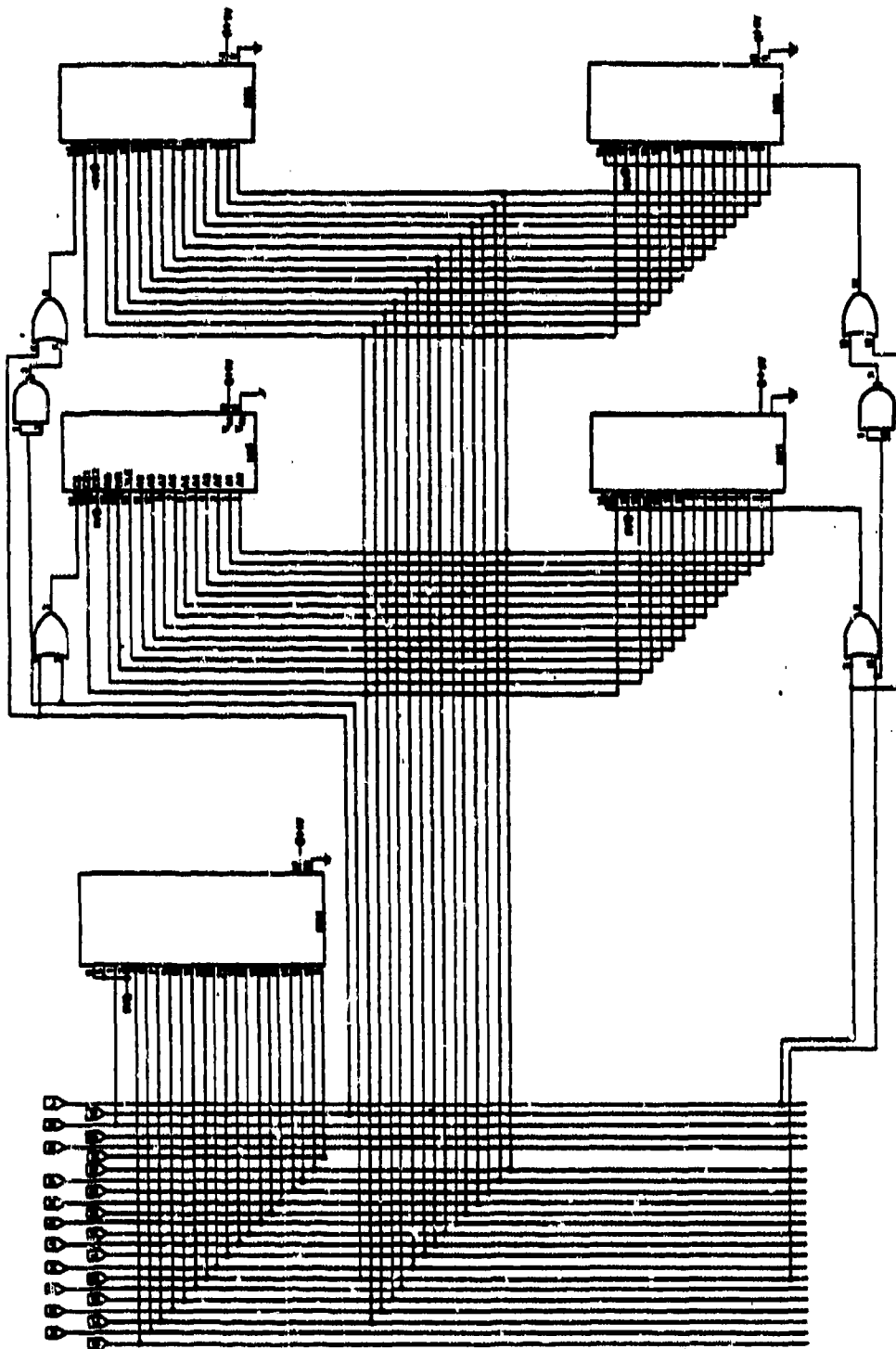


Fig. 29 Schematic diagram for the digital circuit-III

Appendix D
Program Listing

ISIS-II FORTRAN-80 V2.1 COMPILATION OF PROGRAM UNIT MONITR
 OBJECT MODULE PLACED IN CHNMG.OBJ
 COMPILER INVOKED BY: FORT80 CHNMG.FOR WORKFILES(:FO,:FO:):DEBUB

C C THIS IS THE FORTRAN MAIN PROGRAM CALLED MONITR.
 C C IT CALLS SUBROUTINES WRITTEN IN FORTRAN AND 8085
 C C ASSEMBLY LANGUAGE. MONITR AND ITS SUBROUTINES ACQUIRE
 C C DATA FOR THE ANALYSIS, PERFORMS THE PROCESSING, AND
 C C DISPLAYS THE RATE INFORMATION ON THE LCD.

C C ARRAY HEART(960) STORES 12 SEC OF HEART SIGNAL
 C C BREATH(480) STORES 48 SEC OF BREATHING SIGNAL

C C PROGRAM MONITR
 C C IMPLICIT INTEGER(B,H)
 C C INTEGER*1 HEART(960), BREATH(480), FREQ1, FREQ2
 C C INTEGER*1 ITIME1, ITIME2, LIGHT, CHOICE
 C C EXTERNAL GETRDY, DATAIN, DELAY, DOONE, LED, SWITCH
 C C LIGHT=0
 C C NUMB=480
 C C NUMB=960
 C C FREQ1=33
 C C FREQ2=1

C C ITIME1 AND ITIME2 ARE THE PARAMETERS TO DETERMINE THE
 C C SAMPLING FREQUENCIES

C C ITIME1=32
 C C ITIME2=255
 C C NPATE=777

C C CALL THE INITIALIZATION ROUTINE GETRDY
 C C CLEAR THE DISPLAY AND WARNING LIGHTS
 C C SET UP THE "READY" LED TO INDICATE THE COMPLETION OF THE
 C C RESET ROUTINE

C C CALL GETRDY
 C C CALL SWITCH(CHOICE)
 C C IF (CHOICE .EQ. 0) THEN
 C C CALL DISPLY(NPATE)
 C C GO TO 10
 C C END IF
 C C IF (CHOICE .EQ. 1) GO TO 20
 C C IF (CHOICE .EQ. 2) GO TO 35
 C C TAKING DATA FOR THE HEART SIGNAL
 C C CALL DATAIN(FREQ1, HEART(1))
 C C DO 30 N=1, NUMB
 C C CALL DATAIN(FREQ1, HEART(N))
 C C SAMPLING FREQUENCY=80 Hz
 C C CALL DELAY(ITIME1)
 C C CONTINUE

C C THE "READY" LED IS EXTINGUISHED TO INDICATE THE COMPLETION
 C C OF THE DATA ACQUISITION

FORTRAN COMPILER

```

27      CALL DDONE
      C      PROCESSING THE HEART SIGNAL STORED AT HEART(480)
28      CALL RATE(HEART,HRATE,NUMH,BO.O)
      C
      C      IF THE HEART SIGNAL IS TOO WEAK TO PROCESS, THEN WARNING
      C      LIGHT "REPEAT" WILL BE LIT
      C
29      IF (HRATE .EQ. 0) LIGHT=1
30      IF (HRATE .EQ. 999) LIGHT=1
      C      DISPLAYING THE WARNING LIGHTS
31      CALL LED(LIGHT)
      C
32      CALL DISPLY(HRATE)
33      CALL SWITCH(CHOICE)
34      IF (CHOICE .NE. 1) CALL DISPLY(HRATE)
35      GO TO 31
      C      TAKING DATA FOR THE BREATHING SIGNAL
36      CALL DATAIN(FREQ2,BREATH(1))
37      CALL DELAY(235)
38      DO 40 N=1,NUMB
39      CALL DATAIN(FREQ2,BREATH(N))
      C      SAMPLING FREQUENCY=10 Hz
      C      CALL DELAY(11TIME2)
40      CONTINUE
      C
41      THE "READY" LED IS EXTINGUISHED TO INDICATE THE COMPLETION
      C      OF THE DATA ACQUISITION
      C
42      CALL DDONE
      C      PROCESSING THE BREATHING SIGNAL STORED AT BREATH(480)
43      CALL RATE(BREATH,BRATE,NUMB,10.2)
      C
      C      IF THE BREATHING SIGNAL IS TOO WEAK TO PROCESS, THEN WARNING
      C      LIGHT "REPEAT" WILL BE LIT
      C
44      IF (BRATE .EQ. 0) LIGHT=1
45      IF (BRATE .EQ. 999) LIGHT=1
      C      DISPLAYING THE WARNING LIGHTS
46      CALL LED(LIGHT)
      C
47      CALL DISPLY(BRATE)
48      CALL SWITCH(CHOICE)
49      IF (CHOICE .NE. 2) CALL DISPLY(HRATE)
50      GO TO 50
51      END

```

MODULE INFORMATION:

```

CODE AREA SIZE      = GICBH      456D
VARIABLE AREA SIZE = OSBAH      1460D
MAXIMUM STACK SIZE = 0000H      6D
96 LINES READ

```

```

0 PROGRAM ERROR(S) IN PROGRAM UNIT MONITR

```

ISIS-II FORTRAN-80 V2.1 COMPILATION OF PROGRAM UNIT DISPLAY
OBJECT MODULE PLACED IN CHANG6.OBJ
COMPILER INVOKED BY: FORT80 CHANG6.FOR WORKFILES(F01,:F01) DEBUG

MODULE INFORMATION:

```

114D CODE AREA SIZE = 0072H
12D VARIABLE AREA SIZE = 000CH
2D MAXIMUM STACK SIZE = 0002H
22 LINES READ

```

0 PROGRAM ERROR(S) IN PROGRAM UNIT DISPLY

```

ISIS-11 FORTRAN-90 V2.1 COMPILATION OF PROGRAM UNIT RATE
OBJECT MODULE PLACED IN CHAN6.OBJ
COMPILER INVOKED BY: FORTB0 CHAN6.FOR WORKFILES(:F0,:F0:) DEBUS

```

```

1 SUBROUTINE RATE(DATA,HBRATE,NUM,SEFREQ)
2 INTEGER+1 DATA(960),RESULT,IPEAK(480),THRESH
3 INTEGER IADDR(480),HBRATE,RSUM,PERIOD(50),TEMP
4 EXTERNAL COMP8
5
6 THE SLOPE TEST
7 THE POINT IS A PEAK OF A CYCLE IF THE SIGN OF THE SLOPE OF
8 THE SIGNAL CHANGES FROM +VE TO -VE WHEN IT PASSES THROUGH
9 THAT POINT
10
11 M=0
12 DO 300 I=5,NUM-4
13   LSUM=0
14   RSUM=0
15   DO 100 N=I-4,I-2
16     LSUM=LSUM+DATA(N)-DATA(N+2)
17     CONTINUE
18   DO 200 N=I,I+2
19     RSUM=RSUM+DATA(N)-DATA(N+2)
20     CONTINUE
21   IF ((LSUM .LE. 0) .AND. (RSUM .GE. 0)) THEN
22     M=M+1
23     IPEAK(M)=DATA(I)
24     IADDR(M)=I
25   END IF
26 CONTINUE
27 THRESHOLDING
28 I=1
29 CALL COMP8(RESET,IPEAK(I),7)
30 IF (RESULT .NE. 0) THEN
31   M=M+1
32   DO 500 N=I,M
33     IPEAK(N) = IPEAK(N+1)
34     IADDR(N) = IADDR(N+1)
35   CONTINUE
36   I=I+1
37 END IF
38 I=I+1
39 IF (I .LE. M) GO TO 400
40
41 ICTRL=0
42 ICTR=0
43 ICTR=0
44 ICTR=0
45 I=1
46 IF ((IADDR(I+1) - IADDR(I)) .NE. 1) GO TO 450
47 ICTR=ICTR+1

```

```

40      I=I+1
41      IF (I .LT. M-1) GO TO 600
42      IF (ICTR .NE. 0) THEN
43          I=I-ICTR
44          DO 700 N=I, I+ICTR-1
45              CALL COMPB(RESULT, IPEAK(N+1), IPEAK(N))
46              IF (RESULT .EQ. 0) THEN
47                  ICTRL=ICTRL+1
48                  IF (ICTRM .NE. 0) THEN
49                      IF (ICTRL .GE. 1) ICTRL=ICTRL+1
50                      ICTRL=ICTRL-1+ICTRM
51                      ICTRM=0
52                  END IF
53              ELSE IF (RESULT .EQ. 1) THEN
54                  ICTRM=ICTRM+1
55                  IF (ICTRM .NE. 0) THEN
56                      ICTRM=ICTRM-1
57                      ICTRM=ICTRM+1
58                  END IF
59              ELSE
60                  ICTRM=ICTRM+1
61                  IF (ICTRM .EQ. 1) ICTRM=ICTRM+1
62              END IF
63          CONTINUE
64          ICTRM=ICTRM/2+ICTRL
65          IPEAK(1)=IPEAK(ICTRM+1)
66          IADDR(1)=IADDR(ICTRM+1)
67          M=M-ICTR
68          DO 800 N=I+1, M
69              IPEAK(N)=IPEAK(N+ICTR)
70              IADDR(N)=IADDR(N+ICTR)
71          CONTINUE
72          ICTRL=0
73          ICTRM=0
74          ICTR=0
75          ICTR=0
76          END IF
77          I=I+1
78          IF (I .LT. M) GO TO 600
79      C
80      I=1
81      N=IADDR(I)+1
82      M=N-1
83      IF (M .GT. 1) THEN
84          CALL COMPB(RESULT, DATA(N), DATA(N-1))
85          IF (RESULT .NE. 2) GO TO 1300
86          CALL COMPB(RESULT, DATA(N), 0)
87          IF (RESULT .EQ. 0) THEN
88              M=M-1
89              DO 1400 N=I, M
90                  IPEAK(N)=IPEAK(N+1)
91                  IADDR(N)=IADDR(N+1)
92              CONTINUE
93              I=I-1
94          END IF
95          END IF
96          I=I+1

```


FORTRAN COMPILER

```

96 IF (I .LT. N) GO TO 1000
97 N=N-1
98 DO 1500 I=2,N
99 PERIOD(I-1)=IADDR(I)-IADDR(I-1)
100 CONTINUE
101 N=N-1
102 I=1
103 IF (PERIOD(I)-PERIOD(I+1)) 1660,1660,1600
104 TEMP=PERIOD(I)
105 PERIOD(I)=PERIOD(I+1)
106 PERIOD(I+1)=TEMP
107 N=N-1
108 IF (PERIOD(N-1) - PERIOD(N)) 1660,1660,1640
109 TEMP=PERIOD(N)
110 PERIOD(N)=PERIOD(N-1)
111 PERIOD(N-1)=TEMP
112 N=N-1
113 IF (N .GT. 1) GO TO 1620
114 I=I+1
115 IF (I .LT. N) GO TO 1550
116 MEDIAN=(N+1)/2
117 MEDIAN=PERIOD(MEDIAN)
118 I=1
119 IDIFT=IABS(PERIOD(I) - MEDIAN)
120 IF (IDIFT .GT. 5) THEN
121 DO 1800 N=I+1,N
122 PERIOD(N-1)=PERIOD(N)
123 CONTINUE
124 N=N-1
125 I=I-1
126 END IF
127 I=I+1
128 IF (I .LE. N) GO TO 1700
129 ISUM=0
130 DO 1900 I=1,N
131 ISUM=ISUM+PERIOD(I)
132 CONTINUE
133 C
134 IF (N .LE. 0) THEN
135 FRATE=999.0
136 GO TO 2000
137 ELSE
138 SUM=REAL (ISUM)
139 CTR=REAL (N)
140 AVE=SUM/CTR
141 FRATE=SFRED/AVE
142 FRATE=FRATE*60.0
143 END IF
144 HFRATE=NINT (FRATE)
145 RETURN
146 END

```

MODULE INFORMATION:

CODE AREA SIZE = 0738H 1846D
VARIABLE AREA SIZE = 063CH 1596D
MAXIMUM STACK SIZE = 0008H BD
160 LINES READ

0 PROGRAM ERROR(S) IN PROGRAM UNIT RATE

0 TOTAL PROGRAM ERROR(S)
END OF FORTRAN COMPILATION

Appendix E .

Amplitude Response Curves for the Filters

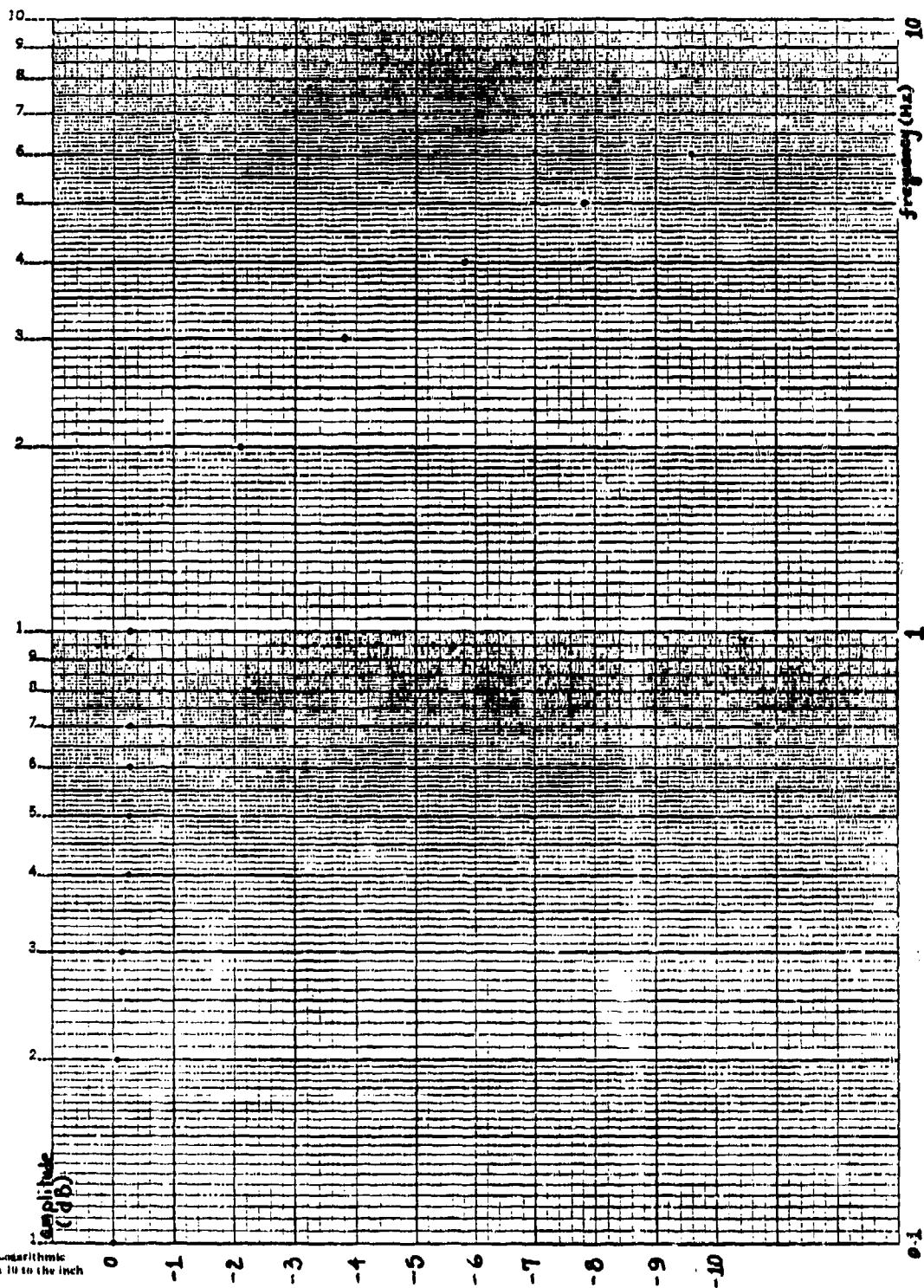


Fig. 30 Amplitude response curve for the low-pass filter
(cut-off frequency = 3.3 Hz)

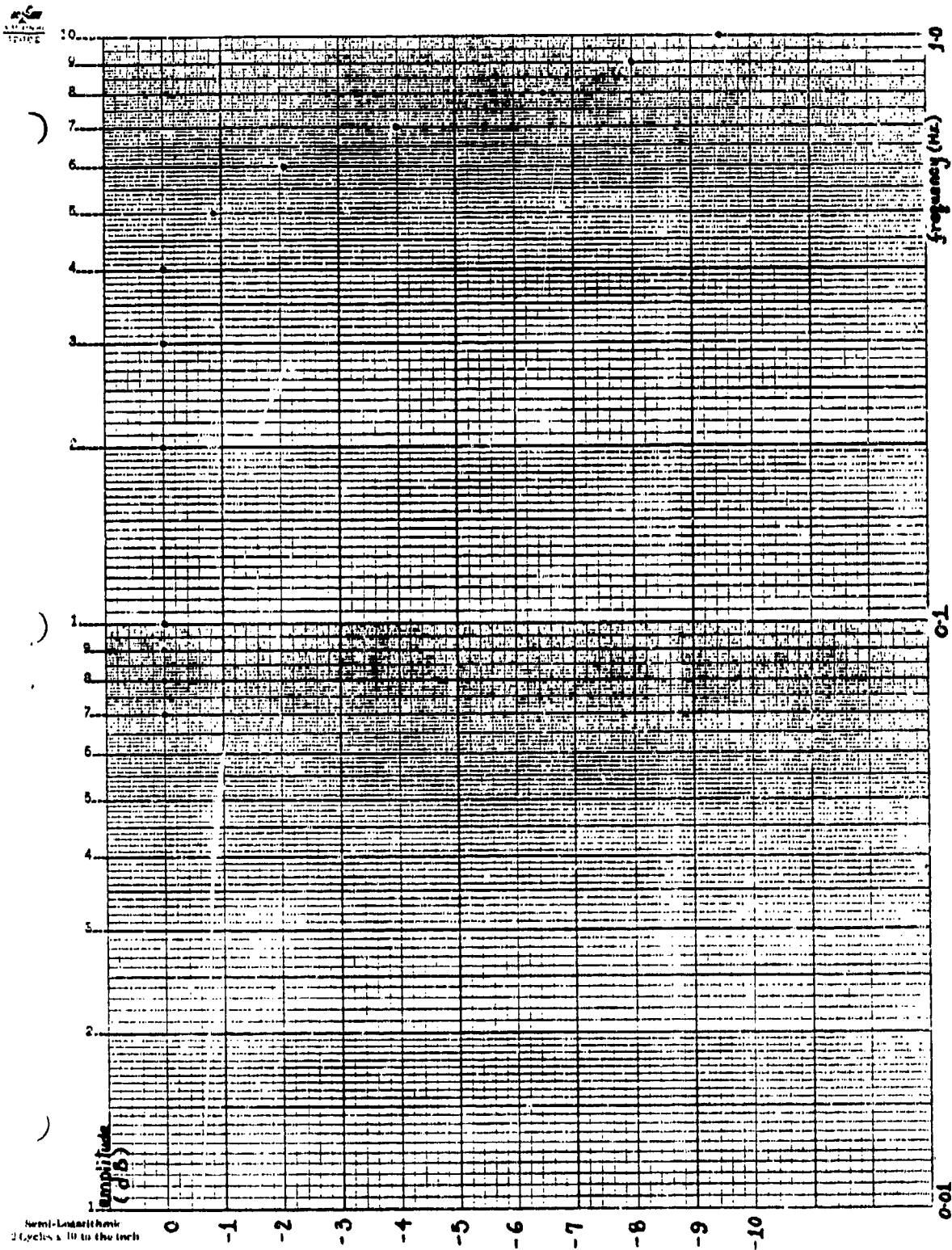


Fig. 31 Amplitude response curve for the low-pass filter
(cutoff frequency = 0.5 Hz)

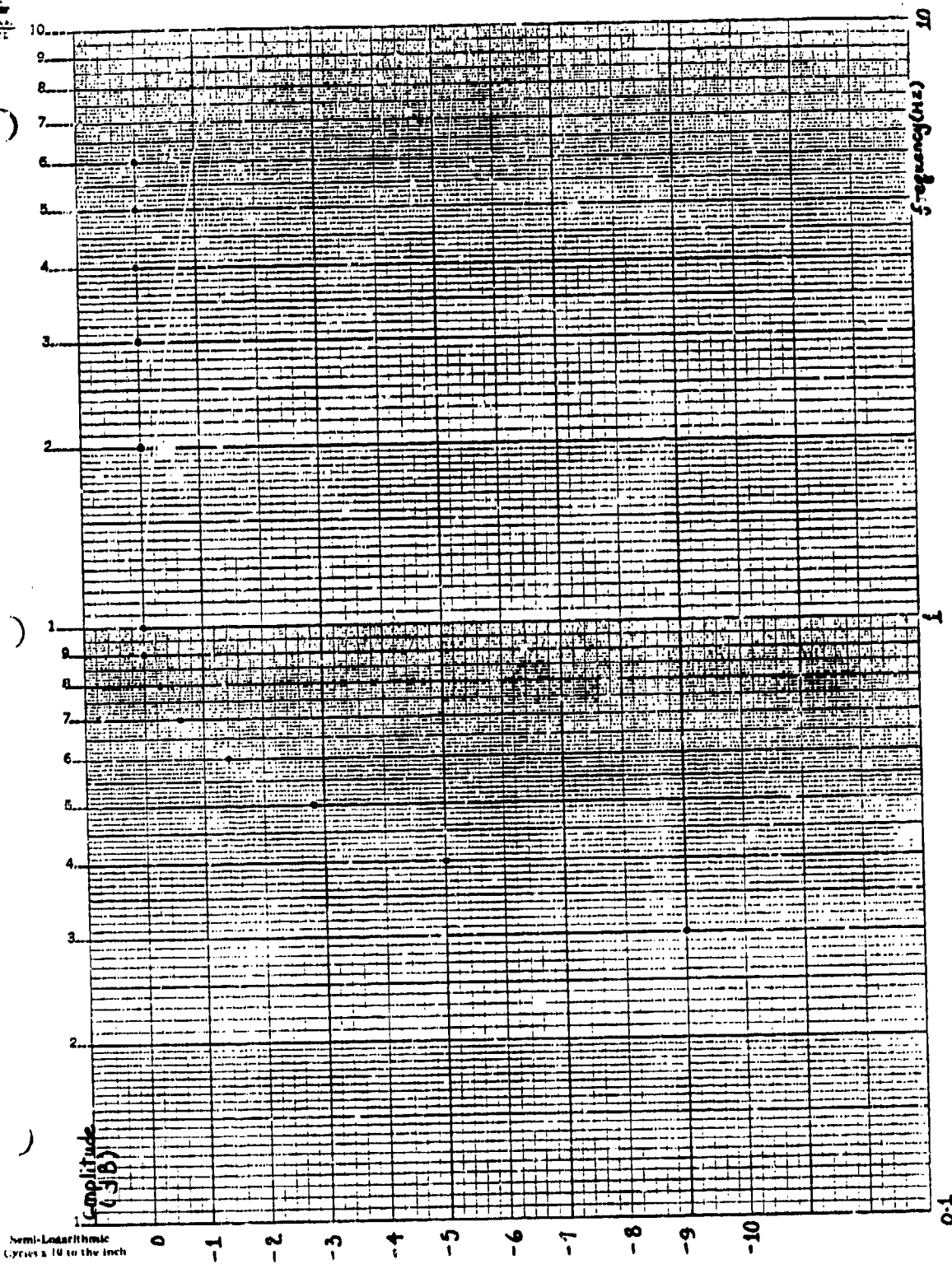


Fig. 32 Amplitude response curve for the high-pass filter
(cut-off frequency = 0.6 Hz)

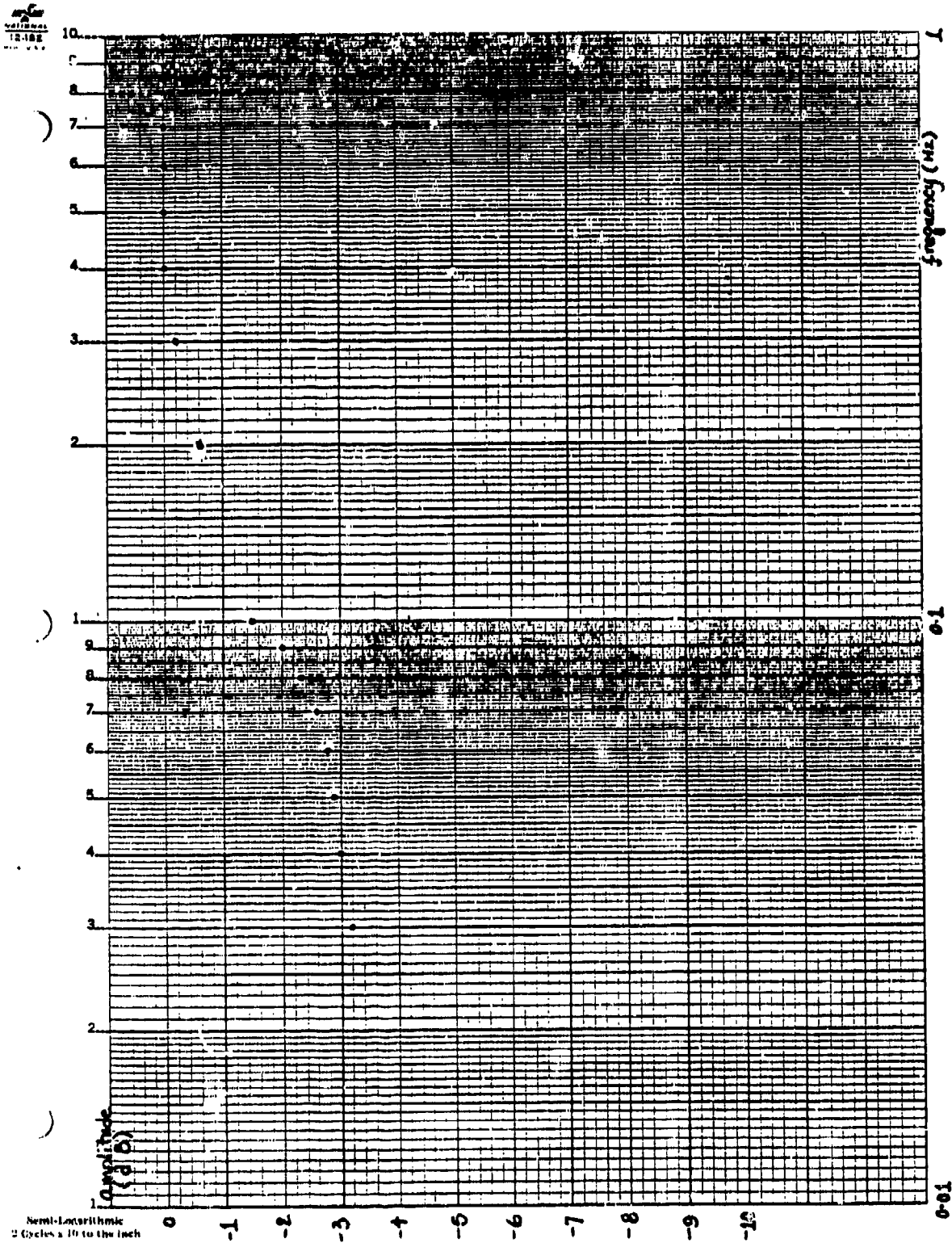


Fig. 33 Amplitude response curve for the high-pass filter
(cut-off frequency = 0.03 Hz)

Unclassified

SECURITY CLASSIFICATION OF THIS PAGE (When Data Entered)

REPORT DOCUMENTATION PAGE		READ INSTRUCTIONS BEFORE COMPLETING FORM
1. REPORT NUMBER BES-5	2. GOVT ACCESSION NO. AD-A16 2 106	3. RECIPIENT'S CATALOG NUMBER
4. TITLE (and Subtitle) Remote Sensing of Body Signs and Signatures		5. TYPE OF REPORT & PERIOD COVERED Final Report 8/1/82-9/30-85
7. AUTHOR(s) J.C. Lin and K.H. Chan		6. PERFORMING ORG. REPORT NUMBER BES-5
9. PERFORMING ORGANIZATION NAME AND ADDRESS Department of Bioengineering University of Illinois at Chicago		8. CONTRACT OR GRANT NUMBER(s) N00014-82-C-0659
11. CONTROLLING OFFICE NAME AND ADDRESS Electromagnetic Radiation Project Office Naval Medical Research and Development Command National Naval Medical Cen., Bethesda, MD 20814		10. PROGRAM ELEMENT, PROJECT, TASK AREA & WORK UNIT NUMBERS
14. MONITORING AGENCY NAME & ADDRESS (if different from Controlling Office) Office of Naval Research 800 North Quincy Street Arlington, Virginia 22217		12. REPORT DATE October 1985
		13. NUMBER OF PAGES 78
		15. SECURITY CLASS. (of this report) Unclassified
		15a. DECLASSIFICATION/DOWNGRADING SCHEDULE
16. DISTRIBUTION STATEMENT (of this Report) Approved for Public Release; Distribution Unlimited.		
17. DISTRIBUTION STATEMENT (of the abstract entered in Block 20, if different from Report)		
18. SUPPLEMENTARY NOTES ← (20)		
19. KEY WORDS (Continue on reverse side if necessary and identify by block number) Doppler Microwaves, Remote Sensing, Noncontact Measurement, Heart Rate, Respiration, Microprocessor-Based, Computer Algorithm, Pattern Analysis		
20. ABSTRACT (Continue on reverse side if necessary and identify by block number) This report describes the development of a microprocessor-based remote sensing system for noncontact detection of heart rate and respiration. Low power sinusoidal microwave signal at a frequency of 10.525 GHz is generated by a Gunn diode oscillator in an integrated Doppler transceiver. A standard gain horn is used to direct the microwave energy to the chest of a subject at a distance of a few centimeters. Since movements associated with the contraction of the heart and expansion of the lungs are translated into		

DD FORM 1 JAN 73 1473

EDITION OF 1 NOV 65 IS OBSOLETE

S/N 0102-LF-014-6601

Unclassified

SECURITY CLASSIFICATION OF THIS PAGE (When Data Entered)

Unclassified

SECURITY CLASSIFICATION OF THIS PAGE (When Data Entered)

motions of the chest wall, the Doppler microwave reflected from the chest is processed to yield information on the frequency and regularity of these cardiopulmonary events.

The microprocessor-based battery-powered system is designed to provide continuous operation for approximately one hour. It allows selection of heart rate or respiration to be displayed on a 3-digit LCD. An analog output jack is provided for oscilloscope display or chart recording. The design range of heart rates is from 40 to 200 beats per minute and that for respiration is from 3 to 30 breaths per minute. The signal acquisition times for heart rate and respiration determinations are 12 and 48 seconds, respectively. Measurements on anesthetized laboratory rats and human volunteers showed good agreement between rates determined with the remote sensing device and conventional techniques, with correlation coefficients greater than 0.98.

request include

Fig 1

S/N 0102-LR 014-6601

Unclassified

SECURITY CLASSIFICATION OF THIS PAGE (When Data Entered)